Elsevier Editorial System(tm) for Catena
Manuscript Draft

Manuscript Number:

Title: Reconsidering the compound effect of geomorphology, vegetation, and climate change on paleopedogenesis in sensitive environments (Northern Apennines, Italy)

Article Type: Research Paper

Keywords: complex paleosols; paleosols sequences; Rock-Eval analysis; soil micromorphology; Northern Apennines; slope dynamic

Corresponding Author: Dr. Anna Masseroli, Ph.D

Corresponding Author's Institution: Universtiy of Milano

First Author: Anna Masseroli, Ph.D

Order of Authors: Anna Masseroli, Ph.D; Sara Villa; Guido S Mariani, Ph.D; Irene M Bollati, Ph.D; Manuela Pelfini, Prof.; David Sebag, Ph.D; Eric P Verrecchia, Prof.; Luca Trombino, Prof.

Abstract: Complex sequences of paleosols are often formed by the interaction between pedogenesis and geomorphological evolution. Their study, particularly in mountain areas, is useful to reconstruct past environmental conditions as well as climate shifts, and to gather information on the morphodynamical processes affecting the landscape through time.
Since the combined role that all different factors can play in the soil formation and evolution through time and space influence the formation and evolution of those complex paleosol sequences, a multidisciplinary study was conducted at the NW slope of Mt. Cusna (Northern Apennines, Italy). This work aims to reconstruct and to evaluate how the interactions between the geomorphological context, the Holocene climate variations, and the modification of the vegetation cover and composition influence the soil development of this area.
A combination of routine soil analyses (i.e., grain-size distributions, total organic carbon, total nitrogen, pH, and Fe/Al extractions), soil micromorphology and the Rock-Eval pyrolysis allowed to characterize and to correlate the different soil units constituting a toposequence of six soil profiles.
The presence of different pedological units that can be correlated along the slope, underlines the occurrence of separate events of pedogenesis, spatio-temporally linked to recognizable stability phases at slope scale. These phases of biostasy, characterized by vegetation cover and soil development, alternate to phases of rhexistasy, characterized mainly by slope instability (i.e., aggradation/degradation).
In detail, in the Mt. Cusna toposequence three different soil units, linked to three different stability phases, have been identified: the earliest stability phase, characterized by the presence of well-developed Luvisols, the subsequent stability phase typified by less expressed Luvisols, and the ongoing stability phase with Leptosols. This latter pedogenetic phase, in some cases, is superimposed to the previous one, so affecting the exhumed paleosols.

In this light, the Mt. Cusna toposequence characterization allowed to enlighten the complexity of soil polygenesis in higher detail than the previous studies, not only reconstructing the past environmental conditions but also inferring the succession of phases of slope stability and phases characterized by erosion and deposition processes.

Suggested Reviewers: Birgit Terhorst
Universität Würzburg, Institute of Geography and Geology Am Hubland 97074 Wuerzburg
birgit.terhorst@uni-wuerzburg.de

Fabio Terribile
Università degli Studi di Napoli Federico II, Dipartimento di Agraria
fabio.terribile@unina.it

Martine Gerard
Sorbonne Université/CNRS/MNHN/IRD,Institut de minéralogie, de physique des matériaux et de cosmochimie
martine.gerard@upmc.fr

Cover letter

UNIVERSITÁ DEGLI STUDI DI MILANO
DIPARTIMENTO DI SCIENZE DELLA TERRA "ARDITO DESIO"

Dear Editors,

I am pleased to submit an original research paper entitled "*Reconsidering the compound effect of geomorphology, vegetation, and climate change on paleopedogenesis in sensitive environments (Northern Apennines, Italy)*" by Anna Masseroli, Sara Villa, Guido S. Mariani, Irene M. Bollati, Manuela Pelfini, David Sebag, Eric P. Verrecchia, and Luca Trombino for consideration for publication in *Catena*.

The research aims at the reconstruction and evaluation how the interactions between the geomorphological context, the Holocene climate variations, the modification of the vegetation cover and composition can influence the soil development, on the NW slope of Mt. Cusna in the Northern Apennines.

The area of Mt. Cusna has already been investigated with an array of studies based on various approaches in order to reconstruct its climate and environmental history through the Holocene (Compostella et al., 2013 published by Quaternary International, Compostella et al., 2014 published by The Holocene, Mariani et al., 2018 published by Journal of Maps and Mariani et al., 2019 published by Catena).

The novelty of this work is the focus on the combined effect that all the above mentioned different soil formation factors have played in soil formation and evolution through time and space.
Furthermore, the Mt. Cusna toposequence characterization allowed to enlighten the complexity of soil polygenesis in higher detail than the previous studies, not only reconstructing the past environmental conditions but also inferring the geomorphological processes that affected the area during the Holocene.

Our findings reveal the presence of different pedological units, whose characterization led to the discovery of a deeper and older unit. These units correlated along the slope, proved to be useful to retrace the occurrence of a succession of phases of slope stability, during which soils developed, and phases characterized by erosion and deposition processes.

The use of different lab techniques improves the knowledge about the soil genesis, additionally our results of Rock-Eval analysis suggest the presence of a relationship between paleosols and organic matter thermal stability opening new research paths in paleopedogenesis.

This manuscript has not been published and is not under consideration for publication elsewhere.

We hope that our work will merit the attention of your Journal.
Thank you for your consideration of this manuscript.
We appreciate your time and look forward to your response.

Yours sincerely,

Anna Masseroli, Sara Villa, Guido S. Mariani,
Irene M. Bollati, Manuela Pelfini, David Sebag,
Eric P. Verrecchia, and Luca Trombino

.

Segreteria Amministrativa
Via L. Mangiagalli, 34
20133 Milano
tel. 02.50315538
fax 02.50315540
segramm.terra@unimi.it

Sezione di Geofisica
Via Cicognara, 7
20133 Milano
tel. 02.50318485
fax 02.50318489

Sezione di Mineralogia
Via S. Botticelli, 23
20133 Milano
tel. 02.50315600
fax 02.50315597

Sezione di Geologia e Paleontologia
Via L. Mangiagalli, 34
20133 Milano
tel. 02.50315499
fax 02.50315494

Highlights

- Different soil units testify the succession of slope stability/instability phases
- Deciphering the complexity of soil polygenesis in high detail
- Rock-Eval analysis enlighten the relationship between paleosols and organic matter
- Environmental conditions reconstruction based on soils and paleosols analysis

Reconsidering the compound effect of geomorphology, vegetation, and climate change on paleopedogenesis in sensitive environments (Northern Apennines, Italy)

Masseroli A.[1], Villa S.[2], Mariani G.S.[3], Bollati I.M.[1], Pelfini M.[1], Sebag D.[4,5], Verrecchia E.P.[4], Trombino L.[1]

1 Department of Earth Sciences "A. Desio", Università degli Studi di Milano, Milano, Italy;
2 Dipartimento di Scienze Agrarie e Ambientali – Produzione, Territorio, Agroenergia (DiSAA), Università degli Studi di Milano, Milano,Italy;
3 Dipartimento di Scienze Chimiche e Geologiche, Università degli Studi di Cagliari, Cagliari, Italy;
4 Institute of Earth Surface Dynamics, Faculty of Geosciences and the Environment, Université de Lausanne, Switzerland;
5 Normandie University, UNIROUEN, UNICAEN, CNRS, M2C, 76000 Rouen, France.

Corresponding author:
anna.masseroli@unimi.it
http://orcid.org/0000-0002-9845-2608
Earth Science Department "A. Desio"
Via Mangiagalli, 34; 20133 Milan - ITALY

Abstract

Complex sequences of paleosols are often formed by the interaction between pedogenesis and geomorphological evolution. Their study, particularly in mountain areas, is useful to reconstruct past environmental conditions as well as climate shifts, and to gather information on the morphodynamical processes affecting the landscape through time.

Since the combined role that all different factors can play in the soil formation and evolution through time and space influence the formation and evolution of those complex paleosol sequences, a multidisciplinary study was conducted at the NW slope of Mt. Cusna (Northern Apennines, Italy). This work aims to reconstruct and to evaluate how the interactions between the geomorphological context, the Holocene climate variations, and the modification of the vegetation cover and composition influence the soil development of this area.

A combination of routine soil analyses (i.e., grain-size distributions, total organic carbon, total nitrogen, pH, and Fe/Al extractions), soil micromorphology and the Rock-Eval pyrolysis allowed to characterize and to correlate the different soil units constituting a toposequence of six soil profiles.

The presence of different pedological units that can be correlated along the slope, underlines the occurrence of separate events of pedogenesis, spatio-temporally linked to recognizable stability phases at slope scale. These phases of biostasy, characterized by vegetation cover and soil development, alternate to phases of rhexistasy, characterized mainly by slope instability (i.e., aggradation/degradation).

In detail, in the Mt. Cusna toposequence three different soil units, linked to three different stability phases, have been identified: the earliest stability phase, characterized by the presence of well-developed Luvisols, the subsequent stability phase typified by less expressed Luvisols, and the ongoing stability phase with Leptosols. This latter pedogenetic phase, in some cases, is superimposed to the previous one, so affecting the exhumed paleosols.

In this light, the Mt. Cusna toposequence characterization allowed to enlighten the complexity of soil polygenesis in higher detail than the previous studies, not only reconstructing the past environmental conditions but also inferring the succession of phases of slope stability and phases characterized by erosion and deposition processes.

Keywords

Complex paleosols, paleosols sequences, Rock-Eval analysis, soil micromorphology, Northern Apennines, slope dynamic

1. Introduction

Soil evolution in active landscapes, such as mountain environments, is mainly influenced and controlled by topography (Zanini et al., 2015). Slope dynamics and instability influence soil formation, development, and preservation: conditions of slope instability can dramatically impact on soil formation and conservation in both short and long terms (Coltorti et al., 2019; Bollati et al., 2019). Areas characterized by steep slopes are affected by frequent and, often, rapid mass movements related to gravity and water-driven processes, which are able to substantially disrupt the relief and modify the old surfaces and dismantling previous soils and paleosols (Dewolf and Bourrié, 2008). Slope processes can vary in frequency and intensity under changing climate and environmental conditions, resulting in a succession of rhexistasy and biostasy phases (Erhart, 1967). Consequently, pedogenesis can be variously impaired over time, whether interrupted, and soils can be buried by deposition phases, or get partially or completely eroded. Moreover, during the successive stability phases, soil formation processes can restart under new environmental conditions. In this light, the result of this tight interaction between pedogenesis and geomorphological evolution is the formation of complex sequences of paleosols, which formed in different morphoclimatic environments associated to distinct paleosurfaces (Coltorti and Pieruccini, 2006; Vittori Antisari et al., 2016). Therefore, an exhaustive investigation of such sequences of paleosols is useful to reconstruct past environmental conditions as well as climate shifts, and to gather information on the morphodynamic processes affecting the landscape through time (Ruellan, 1971; Magliulo et al., 2006; Sheldon and Tabor, 2009). This proxy, evidence of environmental changes recorded in soils and paleosols, is often used as a paleoenvironmental tool in the mountain areas (Kaiser et al., 2007; D'Amico et al., 2016), and specifically in the Apennines (Giraudi, 2005; Magliulo et al., 2006; Coltorti and Pieruccini, 2006).

In the Northern Apennines, the area of Mt. Cusna has been investigated with an array of studies based on various approaches in order to reconstruct its climate and environmental history through the Holocene. Multidisciplinary paleoenvironmental studies carried out at the treeline (Compostella et al., 2013; 2014) helped in characterizing the climate history of the soils in the area. In addition, geoarchaeological investigations of

Mesolithic sites allowed the past environmental conditions of the area to be described using soil data, archaeological evidences, and palynological studies (Biagi et al., 1980; Cremaschi et al., 1984). Two geomorphological maps, within a time distance of 25 years (Panizza et al., 1982; Mariani et al., 2018), were made with the aim of reconstructing the geomorphological evolution of the area through the representation of landforms and paleosurfaces and their reciprocal distribution. However, in the Mt. Cusna area, no studies have been focused yet on the combined role that all different soil formation factors (Jenny, 1941) could have played in soil formation and evolution through time and space.

Therefore, this work aims at the characterization and the correlation of different soil units constituting a toposequence (Milne, 1936) of six soil profiles at the NW slope of Mt. Cusna, by means of a combination of routine soil analyses (i.e., grain-size distributions, total organic carbon, total nitrogen, pH, and Fe/Al extractions), soil micromorphology and a non-conventional approach to interpret soil organic matter dynamics: the Rock-Eval pyrolysis. Moreover, we focused on the information recorded in soils to try to reconstruct and evaluate how the interactions between the geomorphological context, the Holocene climate variations, and the vegetation change influence the formation and evolution of the studied complex paleosol sequences.

2. Materials and methods

2.1. Geological, geomorphological and soilscape settings of the study area

The study area is located on the NW slope of Mt. Cusna (2120 m a.s.l.; Fig. 1a), the second highest peak of the Northern Apennines. Mt. Cusna is located in the territory of Febbio (Emilia Romagna region), inside the "*Parco Nazionale dell'Appennino Tosco-Emiliano*" (Tuscan-Emilian Apennine National Park).

The climate is sub-Mediterranean with abundant and well distributed precipitation (2000 mm/y), with a summer minimum (Compostella et al., 2014). Mean annual temperatures range from 8.8 °C (Ligonchio, 928 m a.s.l., 44°31′N-10°35′E) to 2.2 °C (Mt. Cimone, 2165 m a.s.l., 44°21′N-10°70′E; observation period for both stations 1961-1990). The study area, located between 1600-1700 m a.s.l., is slightly below the current treeline position (1750 m a.s.l., Compostella et al., 2013), and it is characterized by an open deciduous forest dominated by beech (*Fagus sylvatica*). Sparse shrubs and grassland species are also present, mainly *Vaccinium myrtillus*, *Juniperus nana*, *Thymus* sp, and *Laburnum alpinum*.

The bedrock consists mainly of turbiditic sandstones (locally marlstones) with intercalated sequences of claystones and siltstones (Panizza et al., 1982; Bortolotti, 1992). This area was diffusely subject to glacial and periglacial processes during the last glacial phases as testified by the presence of cirques and till deposits in the surroundings and by the general rounded and hilly aspect of the slopes (Losacco, 1949, 1982; Mariani et al., 2018). During the Holocene, the most widespread processes are due to gravity and water runoff (Panizza et al., 1982; Mariani et al., 2018). The Mt. Cusna area is affected by extremely active slope morphodynamics (Bertolini and Pellegrini, 2001) as demonstrated by the presence of rock and debris slides on the slopes of the main ridges, with varying dimensions and positions (Mariani et al., 2018). Moreover, the slope instability is underlined by the presence of colluvium deposits (Mariani et al., 2018).

In the study area, processes related to surface running water play also an important role in shaping the landforms, in different ways, according to the substrate. Runoff and wash out phenomena have low intensity on sandstone outcroppings, due to their semipermeable property. On the contrary, in claystones and marlstones outcropping, water runoff often exposes surfaces due to their mostly impermeable property, and large washout areas are characterized by the presence of pseudo-gullies (Mariani et al., 2018).

Given the widespread presence of degradation processes that have deposited substantial amounts of reworked sedimentary material and have eroded surfaces, the soil landscape is directly affected by the morphological conditions and evolution of the area; consequently, Entisols, Inceptisols, and Spodosols are common (Panizza et al., 1982). Furthermore, the official soil map (Carta Ecopedologica d'Italia 1:250000, Servizi WMS, Geoportale Nazionale, http://www.pcn.minambiente.it/mattm/servizio-wms/) emphasizes the presence of Regosols or Cambisols (IUSS Working Group WRB, 2015) in the study area.

Moreover, in the Mt. Cusna area traces of older soil formation, in the form of relict or buried paleosols, are also found below colluvial deposits; in particular, the most important paleosols associated to the Mt. Cusna paleosurface are located on the northern slope of Mt. Cusna (Panizza et al., 1982). These paleosols have been described as Taptho-Luvisols (Compostella et al., 2014 according to Krasilnikov and Calderón, 2006): these are mature soils, mainly subject to clay illuviation and with well differentiated horizons.

The first traces of human settlements in the area belong to Mesolithic hunters, between Early and Mid-Holocene (Mt. Bagioletto site, 1.6 km N far from the summit of Mt. Cusna; Panizza et al., 1982). Sporadic occupation during Late Holocene to Roman Age was also recorded (Biagi et al., 1980; Panizza et al., 1982; Cremaschi et al., 1984). Later on, historical sources show progressive colonization of the area since the High Medieval Times, with communities surviving on livestock and forest exploitation. Agriculture played a minor role and was limited to small patches nearest to settled villages (Panizza et al., 1982). In present times, farming arrives at 1000-1300 m a.s.l., while pasture reaches higher altitudes. In addition, forested areas were recently destroyed to build tourist facilities.

2.2. Soil sampling

Six soil profiles were dug and described according to Jahn et al. (2006; Table 1) along an altitudinal transect on the NW slope of Mt. Cusna (Fig. 1b). Five soil profiles were chosen in an area as they were affected by running water erosion, whereas one soil profile (04) was excavated in a stable area with a forest plant cover. The locations of the five profiles were chosen on high topographic position, currently preserved from erosion processes. The coordinates of each profile were recorded using a GPS device. Between 0.5 to 2 kg of material were sampled from all identified soil horizons for laboratory analyses (Avery and Bascomb, 1982; Gales and Hoare, 1991; Cremaschi and Rodolfi, 1991). Seven undisturbed samples were collected using Kubiëna boxes (Kubiëna, 1953) from selected soil horizons to obtain thin sections for micromorphological investigations.

2.3 Soil analyses

Air-dried soil samples were treated by wet sieving in order to separate skeleton particles (> 2mm) from the fine earth. The pH (in 1:2.5 soil: distilled water), total Organic Carbon (Org. C) content (Walkley and Black, 1934), and total nitrogen content (Kjeldahl, 1883) were measured for each soil sample. Particle size distributions were obtained on samples pretreated with H_2O_2 (130 volumes); sand fractions (from 2000 to 63 μm) were collected by sieving, while silt and clay particles (< 63 μm) were measured by aerometry with the Casagrande aerometer (Casagrande, 1934).

Different iron and aluminum forms were quantified (Ministero delle Risorse Agricole Alimentari e Forestali, 1994). Non-silicate forms ("free" iron, Fe_d and Al_d) were extracted with a bicarbonate-dithionite-citrate buffer, iron and aluminum in amorphous oxides and hydroxides ("active" forms, Fe_o and Al_o) were extracted with acid ammonium oxalate and, iron and aluminum bound to organic matter with covalent or partially polar bond (Fe_p and Al_p) were extracted in a solution of sodium pyrophosphate. For all forms, the amount of solubilized iron and aluminum in the supernatant was determined by means of a 4100 MP-AES (Agilent), after appropriate dilutions. Data with a %RSD (Relative Standard Deviation) of concentration > 3.5 and/or with a not detectable clear peak, were considered invalid (n.d. in Table 2), while the data close to the detection limit of the instrument were approximated to the minor concentration detectable (<n in Table 2).

In order to compare the results of iron and aluminum extractions to soil characteristics, both iron activity index (Fe_o/Fe_d) (Rhodes and Sutton, 1978) and illuviation (podzolization) index ($Al_o+½Fe_o$) were calculated (IUSS Working Group WRB, 2015). Moreover, the amount of crystalline iron oxides (Fe_{cry}) was calculated as the difference between the dithionite- and the oxalate-extractable Fe ($Fe_{cry}= Fe_d-Fe_o$) (Bascomb, 1968; Pawluk 1972; Cremaschi and Rodolfi, 1991; Zanelli et al., 2007).

Rock-Eval pyrolysis analysis was performed using a Turbo model Rock-Eval® 6 pyrolyser (Vinci Technologies, France). About 60 mg of crushed material, previously sieved (<2mm), was analyzed for each horizon. Total Organic Carbon (TOC), Mineral Carbon (MINC), Hydrogen (HI) and Oxygen (OI) Indices were calculated by integrating the amounts of Hydrocarbon Compounds (HC), CO, and CO_2 produced during thermal cracking of Organic Matter (OM), between defined temperature limits (Lafargue et al., 1998; Behar et al., 2001). The I-index and R-index were computed according to Sebag et al. (2016). Previous studies show both indices are highly correlated along a constant line ("humic trend") in undisturbed soil profiles (Albrecht et al., 2015; Matteodo et al., 2018; Schomburg et al., 2018, 2019; Sebag et al., 2016). For comparison, we used the Matteodo's dataset composed of 46 soil profiles selected across various ecounits in Swiss Alps (Matteodo

et al., 2018). The “humic trend” equations in the I-index/R-index plot was calculated starting from both Matteodo's dataset and study area datataset (colored dots in Fig. 4b).
Finally, a Delta I index was calculated: it refers to the difference between the I-index value of each sample and the I-index value calculated with the “humic trend” equation (in bold in Fig. 4b), calculated starting from study area sample data, at the R-index value of each sample.

2.4 Micropedology

Uncovered soil thin sections were prepared from undisturbed samples through impregnation with polystyrene. Thin sections were then observed by means of a petrographic microscope (Leica Laborlux 18 POL), in parallel (PPL), cross-polarized (XPL), and oblique incident light (OIL), using different objectives (1.6x, 4x, 10x and 25x). Thin sections were described according to Stoops (2003). The interpretation of thin sections was performed according to Stoops et al. (2018).

3. Results

3.1. Soil profiles description and analyses

All the soil profiles are located between 1600 and 1700 m a.s.l. (Fig. 1b); five soil profiles (01; 02; 03; 05; 06) are located in areas affected by running water erosion (Table 1). The vegetation cover is composed of semi-deciduous shrubs in all the area of soil profiles, except for profile 04 characterized by beech forest.

Total depths for all profiles range from around 50 to about 200 cm. The thickest profiles are characterized by the presence of two (01) or three (02, 06) distinct soil units, identifiable in the field by the presence of grain-size discontinuities or buried organic horizons, and/or a color change. Soil structure is moderately expressed by granular or subangular blocky aggregates. Sometimes, surface horizons (i.e., 05 A, 06 O and 06 OA) exhibit only a single-grained structural condition. On the contrary, well separated angular aggregates can be found in buried horizons. Colors range between 10YR and 2.5Y in their hue, with a tendency for chroma to increase with depth inside each single soil unit (see Appendix A for detailed data). All the profiles are characterized by acidic conditions ranging from pH 4 to 5.6, usually increasing with depth, except for surface O horizons, which are often less acid than the underlying horizon (Fig. 2).
Particle size distributions of the investigated soil profiles display some common traits. Silt is always the predominant fraction, ranging from 44% to about 65%, with variable amounts of clay (from 21% to 52%). On the contrary, gravels never exceed 5%, while sands are only rarely > 20% (Fig. 2). Moreover, the grain size distributions allow the presence of different soil units to be confirmed. Indeed, the 01 and 06 soil profiles show an increase in clays at the top of the buried units (e.g., in profile 01: clay increases by 13.2% between horizons BC and 2AB1; in profile 06: clay increases by 13.7% between horizons OA and 2AB1); on the contrary, the 02 soil profile displays an increasing clay content by 2.6% between the horizons 2AB and 2Btg. 03 and 05 profiles are characterized by a clay peak in the B horizons, whereas a peak of coarse materials clearly appears

in correspondence of the topographic surface (03 OA and 05 A) and the deepest (03 BC) horizons (see Appendix B for detailed data and Appendix C for cumulative particle size distribution curves). Lastly, the 04 soil profile, under a stable forested area, shows an increase of the coarse fractions (gravel and sand) all along the profile to the detriment of the clay component (Fig. 2).

The identified discontinuities are also marked by the results from chemical analyses. Indeed, a peak of total organic C content is found at the top horizon of each buried unit in correspondence of the above-mentioned discontinuities: 01 2AB1, 06 3AB, 02 2AB, and in the horizon 02 3AB, while in the horizon 06 2AB1 a total N peak is found (Fig. 2). Conversely, in profile 04, total organic C decreases from the surface horizon with depth, as expected in conventional soil profiles. The same trend can be observed in profiles 03 and 05, with the exception of the OB horizon of 03, which shows an increase in total organic C, and the A horizon of 05, which has a more marked decrease in total organic C than the deeper horizons (Fig. 2).

In the analyzed soil profiles, the total N content follows roughly the same trend as the total organic C (Fig. 2), but with significantly lower values. In surface horizons, total organic C ranges between 14.7 g/kg (02) and over 100 g/kg (04 and 05), while total N content never exceeds 7.0 g/kg. When focusing on superficial OM-rich horizons, the highest total N contents (about 7 g/kg) are found in 01, 04 and 06, while the lowest values belong to 02 (about 1.4 g/kg), following the same trends as total organic C.

The total content of free iron oxides (Fe_d) in four horizons (01 2AB2, 03 OB, 05 ABt2 and 06 2AB1) exceeds 30 g/kg but this parameter generally ranges between 10 and 20 g/kg (Table 2). The values of amorphous iron oxides (Fe_o) tend to be lower (<0.90 - 15.73 g/kg), as well as iron bound with organic matter (Fe_p), which ranges between <3.00 and 15.98 g/kg. Regarding the aluminum content, its values are lower and less variable than those of iron, with the exception of aluminum bound with the organic matter (Al_p) (Table 2). Free aluminum oxides (Al_d) reaches abundance from 2.64 to 5.83 g/kg, amorphous aluminum oxides (Al_o) from 0.85 to 5.59 g/kg, and the aluminum bound with the organic matter (Al_p) from 2.98 to 12.09 g/kg. The crystalline iron oxides (Fe_{cry}) are mainly concentrated in the B horizons (Fig. 3), and the highest value is found in the 05 ABt2 (21.08 g/kg). Along the profiles, the amorphous iron oxides (Fe_o) follow a different trend compared to the trend of crystalline iron oxides (Fig. 3), except for some superficial horizons (e.g., 06 OA) and in a few buried organic horizons (e.g., 01 2AB2). Indeed, in most of the profiles, the amorphous iron oxides show the lowest concentrations in Bt, Btg and partially in Bw horizons (Table 2; Fig. 3). The iron activity index ranges from 0.18 to 0.66. In more detail, its lowest values are found in the Bt, Btg and Bw horizons (Table 2), in particular, in the B horizons of buried soils (e.g., 01 2Bt, 06 2Bw2 and 06 2Bw3). Instead, the BC horizons show the highest values of the iron activity index (e.g., 02 BC, 03 BC).

Finally, the results of the podzolization index ($Al_o + ½ Fe_o$) meet the conditions for the presence of some podzolization processes only in the profile 02 (ABt2 and BC horizons; Table 2).

Rock-Eval indices and parameters (Fig. 4) show that all the superficial organic horizons are plotted at the top left of the HI/OI diagram (Fig. 4a), whereas the buried soils are located at the bottom right of the diagram. Moreover, in the I-index/R-index diagram (Fig. 4b) the superficial organic horizons correspond to low R-index values and high I-index values and are located at the top left of the I-index/R-index diagram, whereas the organo-mineral and mineral horizons have a R-index values > 0.65 and are located in the right portion of the diagram. Taking into consideration the organo-mineral and mineral horizons in the I/R diagram, two different trends can be recognized. A first trend groups the horizons belonging to the superficial units of the soil profiles, which have I-index values varying between -0.3 and 0 (colored dots in Fig. 4b), whereas a second trend groups the horizons belonging to the buried units, which have higher I-index values, ranging from -0.2 to 0.5 (colored diamonds in Fig. 4b), except for horizons 01 2AB1, 2AB2 and 06 2AB1, 2AB2. On the other hand, some horizons from the superficial units are characterized by high I-index values (02 BC, ABt1 and ABt2; 04 Bt, Btg, AB; 03 BC). Moreover, when comparing R-index with depth, buried soils evidence a different trend; indeed, the 01 buried soil display R index values higher than the 02 buried soil, at the same depth and with similar TOC contents (fig. 5a,b). The presence of two different trends can also be observed when taking into consideration the I-index/TOC diagram: the horizons belonging to the first trend show an expected increase of the I-index with TOC and a decrease with depth, whereas the horizons belonging to the second trend have (i) high I-index values even with low TOC and (ii) I-index values which are not decreasing with depth (Fig. 5c, d). Finally, horizons belonging to the second trend have high delta I values (Fig. 5e).

3.2. Soil thin sections micromorphology

The micromorphological observations were carried out on four out of the six examined profiles: 01, 02, 04 and 05 (see Appendix D for detailed thin sections descriptions). Horizons 02 ABt1, 01 2Bt and 04 Bt show some similar features: they all are characterized by granular aggregates of fine material and angular-subangular blocky aggregates, together with Fe-Mn nodules and well-developed clay coatings. Moreover, in the 02 ABt1, reworked soil fragments of subangular aggregates of fine material (i.e., pedorelicts *sensu* Brewer, 1976) with a high degree clay illuviation, and few allochthonous weathered rock fragments are present (i.e., lithorelicts *sensu* Brewer, 1976). Furthermore, regarding the coarse mineral fraction, there are similar proportions of sandstone and claystone fragments in 02 ABt1 and 04 Bt, while in the 01 2Bt sandstone constitutes the prevalent lithology of fragments.

Similarly, 01 2AB1 and 2AB2, 05 ABt1 and ABt2 and 04 Btg horizons show analogous characteristics, such as their complex microstructure including granules and reddish clayey subangular aggregates, which contain a high proportion of Fe-Mn nodules (Fig. 6a, b). Moreover, the 01 2AB1 horizon differs from the 2AB2 horizon by the predominant sub-angular aggregates in the latter. Finally, in the 05 ABt1 and ABt2 and 04 Btg horizons show the presence of clay illuviation features (coatings); in the latter horizon, hydromorphic features in the form of depletion pedofeatures and intercalations are also found.

The micromorphological approach further underlines the presence of peculiar characteristics in 01 A2, BC and 2AB1 and 02 2Btg horizons. For example, the 02 2Btg horizon exhibits a compact, vughy microstructure, and, well-developed diversified pedofeatures, such as dense digitate Fe-Mn nodules, typic clay coatings, typic clay infillings, and Fe-Mn hypocoatings (Fig. 6c, d).

Otherwise, the 01 A2, BC and 2AB1 horizons show a twofold distribution of crumbs and reworked subangular aggregates reddish in color, and characterized by a high degree of pedogenesis (i.e., pedorelicts *sensu* Brewer, 1976). These pedofeatures are more common in the BC horizon (Fig. 6e, f). Finally, 01 2AB1 and 2AB2 contain identifiable pedofeatures only as Fe-Mn nodules, which are more concentrated inside the subangular reworked soil fragments.

4. Discussion

4.1. Complex paleosol sequences and the characterization of buried units

Sedimentological and chemical data help in identifying the presence and in defining the boundaries of the soil units recognized in the field. Trend anomalies detected in analytical values are found in profiles 01 (between horizons BC-2AB1), 02 (between horizons BC-2AB and 2Btg-3AB), and 06 (between horizons OA-2AB1 and 2Bw3-3AB; Fig. 2). In horizons 2AB1 of 01, 2AB1 and 3AB of 06, high values of total organic C or total N contents as well as of fine material, underline the presence of paleosurfaces, subsequently buried by coarse colluvial deposits, which disconnected the soils from surface pedogenetic processes. On the contrary, it is not possible to identify precisely in profile 02 the paleosurface location at the top of the 2AB horizon from the colluvial material above it. Even if the organic matter content peaks in 2AB horizon, both 2AB and BC horizons possess a high percentage of sand and gravel (Fig. 2). Moreover, both horizons in the field have a homogeneous aspect: it is possible that the distinction between these two units may be difficult to identify because of a higher energy of deposition of the colluvium, which mixed part of the materials during the process. In the same profile, the total organic C content allows a discontinuity at the top of the 3AB horizon to be identified (Fig. 2). The variations in particle size distributions within profiles 03, 04 and 05 are not attributed to the presence of paleosurfaces.

Micromorphological observations of thin sections from 01 and 02 profiles provide further information about the presence of different soil units and their respective characteristics. In 01, the presence of two distinct units is highlighted by the nature of the coarse material: in the surface unit (unit I) fragments of claystones are more abundant while in the deeper one (unit II), fragments of sandstones are more common. This difference in the coarse fraction lithology likely indicates the occurrence of two different parent materials, separating clearly two soil units. In unit II, weathering processes occurred in oxidative conditions with water infiltration, emphasized by the yellowish color of the groundmass indicating the presence of iron hydroxides (Sauro et al., 2009; Stoops et al., 2010, 2018; Compostella et al., 2014). The presence of clay illuviation features, indicated by clay coatings found in the 2Bt horizon, requires alternating phases of water infiltration into the soil, in order to permit clay translocation into the deep horizons (McCarthy et al., 1998; Stoops et al., 2010, 2018). Moreover, the presence of Fe-Mn nodules indicates temporary waterlogging conditions inside the soil (McCarthy et al., 1998; Stoops et al., 2010, 2018). The diffuse and irregular boundary of the nodules witnesses their *in situ* formation, without evidence of transport from other locations (Fedoroff and Goldberg, 1982). In unit I, frequent blocky peds show a generally reddish micromass color associated to Fe-Mn nodules, which indicate a degree of weathering greater than in the surrounding soil groundmass: therefore, these blocky peds can be regarded as pedorelicts (*sensu* Brewer, 1976), i.e., reworked fragments of an older soil (Fig. 6e, f) redeposited within more recent horizons (Cremaschi et al., 2018; Kemp, 1998; Nicosia, 2006; Rellini et al., 2007; Sauro et al., 2009). Moreover, these reworked fragments of paleosol are similar, in terms of fabric, to the 2AB2 horizon; thus, it is reasonable to state that they were eroded from higher portions of the slope and deposited within the presently BC horizon.

Regarding 02 profile, the micromorphological analysis indicates that the unit II (e.g., 2Btg horizon) is characterized by a stronger degree of pedogenesis than the unit I (e.g., ABt1 horizon). This is probably due to a greater intensity and/or duration of a pedogenetic phase. In unit II, clay coatings are clearly visible (Fig. 6c, d) and it is often possible to identify an orientation in the deposition of fine material due to the development of crescent internal fabric. This corroborates the hypothesis of transport of clay materials from upper horizons (McCarthy et al., 1998). Moreover, the 2Btg horizon is the only one showing the development of Fe-Mn hypocoatings, due to longer periods of waterlogging (McCarthy et al., 1998; Stoops et al., 2010). Finally, only rare reworked paleosol fragments (pedorelicts *sensu* Brewer, 1976), composed of clayey blocky peds, are found in the ABt1 horizon.

4.2. Correlation of soil units

As already described in section 4.1 of the Discussion, the studied toposequence is constituted by six soil profiles located at different altitudes along the NW slope of Mt. Cusna, chosen according to their topographic position. Among the analyzed soil profiles, three are composed of different units, whereas only one soil unit is present in the other three profiles (03; 04 and 05).

In the following section, the most widespread unit set (i.e., unit II of 01; unit I of 02; 03; 04; 05; unit II of 06) is first characterized in order to better correlate the various soil profiles (Fig. 7). Indeed, the unit II of 01 (e.g., 2Bt) and the unit I of 02 (e.g., ABt1), although characterized by a different mineral component, are associated with the presence of clay illuviation and a very similar microstructure, together with the presence of moderately impregnated amorphous nodules. Therefore, these units could be formed by the same pedogenetic event on different parent materials, the latter deposited by distinct colluvial events.

Unit II of 01 can also be correlated with 05 profile (e.g., ABt1 and ABt2), which shows similar aggregates (both subangular blocky and granular) and microstructure with regard to the horizons 2AB1 and 2AB2 (01 profile), as well as clay illuviation features in the horizon 2Bt (01 profile). Moreover, moderate impregnative amorphous nodules of Fe-Mn are present through the referred horizons. The same consideration regarding microstructure, clay illuviation features, and amorphous nodules can be extended to the 04 profile, even if, in the horizon 04 Btg, the presence of hydromorphic features (i.e., depletion pedofeatures and intercalation, *sensu* Fedoroff and Courty, 2012) underlines a further pedogenetic phase induced by water logging, probably due to the topographic position.

The sedimentological and chemical data allow the above described correlation based on micromorphological features to be extended (Fig. 7): the unit II of the 01 (e.g., 2AB1 and 2AB2) and 06 (e.g., 2AB1 and 2AB2) profiles show the same clay high and sand low contents, and similar values of total organic C and total N contents. On the other hand, 03 profile can be correlated to the unit I of 02, not only because both units are characterized by a very low total organic C and total N contents, but also for their relative position along the slope.

In two profiles, 01 and 06, the above correlated unit is overlain by soil horizons, pointing to another soil unit (Fig. 7). This surficial unit, even if it is thin, shows uniform soil characteristics (particle size distributions, total organic C and total N contents), and could therefore be related to the same pedogenetic phase.

Focusing on soil horizons underlying the above correlated unit, the micromorphological observations highlight a general greater weathering impact. The 02 2Btg horizon (unit II) has very few analogies with the horizons observed in other profiles: the presence of well-developed pedofeatures (i.e., dense digitate nodules of Fe-Mn, typic clay coatings, typic clay infillings; and Fe-Mn hypocoatings) testifies a more intense pedogenetic phase, followed by a secondary hydromorphic phase induced by waterlogging. Moreover, the peculiarity of this unit II is also underlined by the organic matter thermal signature: in the R-index/depth plot, horizons of unit II from 02 have a lower R-index compared with the horizons belonging to unit II from 01, which are located at the same depth (Fig. 5b), due to a presence of different proportion of the most refractory and persistent organic matter fraction (related to pedogenetic and inherited contributions) in the two units. A similar trend, though not so marked, is also visible in the R-index/TOC plot (Fig. 5a), where the horizons belonging to unit II of 02 are separated from the others. Furthermore, unit II of 02 may be correlated to unit III of 06 (Fig. 7). This deepest unit of 06 is only represented by a single horizon (3AB), but its stratigraphic continuity, in addition to Rock-Eval analysis results, suggest a possible correspondence between this unit and unit II of 02. Horizon 06 3AB is always located close to the horizons belonging to unit II of 02 in both R-index/TOC (Fig. 5a) and R-index /depth plots (Fig. 5b), underlining similar organic matter dynamics.

Regarding Rock-Eval results, as discussed above, the HI/OI diagram emphasizes the way horizons belonging to unit II of 01 (red dots, 2AB1, 2AB2 in Fig. 4a) and unit II of 06 (violet dots, 2AB1, 2AB2 in Fig. 4a) group in the same set as the present-day surface horizons of all the profiles, while units II of 02 and III of 06 are located at the bottom right of the plot, probably due to the presence of more stable OM. These horizon groupings are clearly distinguishable observing the results of cluster analysis (Fig. 8) carried out on the Rock-Eval indices take into consideration (HI, OI, R-Index, I-Index): in the dendrogram it is possible to observe how the organic O horizons clearly differ from the organo-mineral and mineral horizons. Among the organo-mineral and mineral horizons, the horizons belonging to unit II of 01 and unit II of 06 group are grouped in the same set as the present-day surface horizons of all the other profiles (02,03,04 and 05), while units II of 02 and III of 06 are all grouped together, close to the deepest horizons of the other units (01 2BC2; 02 BC, ABt2; 04 Bt, Btg; 06 2Bw3) (Fig. 8). Moreover, the cluster analysis grouped the organo-mineral and mineral horizons in two different great groups, which can be attributable to a different evolution trend of organic matter. Indeed, in the graph of I/R indices (Fig. 4b), the #*B* horizons belong to the first set (i.e., 01 2Bw, 2Bt, 2BC1, 2BC2; 02 BC, 2AB, 2Btg, 3AB; 03 BC; 04 AB, Bt, Btg; 06 2Bw1, 2Bw2, 2Bw3, 3AB; colored diamonds in Fig. 4b; these horizons are not belonging solely to buried units) show a new trend, parallel to the "*Inherited Organic Matter Trend*" proposed by Sebag et al. (2016). On the other hand, horizons richer in organic matter (i.e., 01 A1, A2, BC, 2AB1, 2AB2; 02 OB; 03 OA, OB; 04 OA; 05 A, ABt1, ABt2; 06 OA, 2AB1, 2AB2; colored dots in Fig. 4b; these horizons belong to surface or buried units) fit the "*Humic Trend*" (Sebag et al., 2016; Matteodo et al., 2018).

This new identified trend, grouping #*B* horizons with a high degree of weathering observed in both surface and buried units, suggests the presence of a relationship between these different soil horizons. In these horizons, as already stipulated, the presence of features related to pedogenetic processes not in equilibrium with the present-day environmental conditions, clearly defines these soil horizons as parts of paleosols. Moreover, this new trend clearly differs from the "*Humic trend*" (Sebag et al., 2016; Matteodo et al., 2018), mainly for what concerns the I-index values (Fig. 5c,e). Indeed, the horizons belonging to this trend show high I-index values (even if the TOC content is low; Fig. 5c,e), emphasizing the presence of immature organic matter. This peculiarity of the trend supports the hypothesis that these soils located along the trend are paleosols. The presence in these horizons of high I-index values allows these horizons to be identified as organic ones, probably located in the past at the surface, whereas the presence of low TOC contents, unusual for organic horizons, is explained when considering the geomorphological context of the area. The contribution of mineral material, especially in the superficial horizons, is due to colluvium deposition episodes affecting the slope, contributing to organic matter dilution, and, at the same time, burying soil units, isolating the soil by preventing the modification and external contributions to the buried organic matter.

Two type of paleosols can be observed: (i) buried paleosols (i.e., 01 2Bw, 2Bt, 2BC1, 2BC2; 02 2AB, 2Btg, 3AB; 06 2Bw1, 2Bw2, 2Bw3, 3AB), as considered soil units are buried, and (ii) exhumed paleosols (i.e., 02 ABt1, ABt2, BC; 03 BC; 04 AB, Bt, Btg), when considered soil units outcrop at the surface. Therefore, the new observed trend in the I/R plot identifies some horizons of maximum weathering in the paleosols, regardless their morphological position, within the given limits of the study area. This specific paleosols trend in the I/R plot represents a potential approach for further investigations regarding new criteria for paleosols identification.

Finally, regarding the iron and aluminum content, all analysed Bt, Btg and Bw horizons show an increase in crystalline iron oxides (Fe_{cry}), underlining the expression of some pedogenesis at work (Table 2; Fig. 3). Furthermore, the iron activity index (Fe_o/Fe_d) shows a decrement within the most mature Bt, Btg and Bw horizons, likely emphasizing a stronger weathering (Table 2). Unfortunately, this ratio does not change significantly when comparing recent soils and paleosols; consequently, it is not wise to use it as a proxy for soil age (Arduino et al., 1986). The reasons for this are that paleosols are relatively young and that the mixing caused by colluvium contributes to blur the soil message, as testified by the presence of pedorelicts and lithorelicts (*sensu* Brewer, 1976).

4.3. The role of geomorphological processes in the development of complex pedosequences

The presence of different pedological units, and their correlation along the slope, underlines the occurrence of separate events of pedogenesis, spatio-temporally related to recognizable stability phases at the slope scale. These phases of biostasy (Erhart, 1967) are characterized by the absence of erosion and/or deposition on the slope, a vegetation cover, and a soil development. They alternated with phases of rhexistasy (Erhart, 1967), characterized by slope instability. The study area has been affected by various colluvial events, as testified by trends in coarse materials content and the presence of pedorelicts and lithorelicts (*sensu* Brewer, 1976) in the surface units.

Moreover, the phases of rhexistasy strongly control the conditional conservation of soils along the slopes: higher energy conditions would produce excessive disruption along the slopes in form of increased colluvial and landslide events. These events would destroy the soil cover and cause the disappearance of evidences of previous pedogenetic phases in the area and at the same time inhibit the formation of new soils. Consequently, only moderate energy phases are assumed in the study area. However, even if these moderate multiple phases of slope activity may have locally eroded part of the pre-existing soil cover (e.g., unit I of 02), at the same time, they locally buried parts of it, preserving some paleosols over time (e.g., unit II of 01). In addition, the geomorphological evolution of the slope through time may also brought previously buried paleosols to the surface again, superimposing a new pedogenetic phase on pre-altered materials, as attested by unit I of 02 and probably 03 and 05. In this sense, slope morphodynamics do not seem to influence directly the intensity of *soil formation processes*, but they act as a key factor controlling the distribution and occurrence of soil units and paleosols. Therefore, the development of the studied complex pedosequences is not the exclusive result of vertical top-down processes but of a number of complex processes including near-surface processes such as material sedimentation and erosion.

On account of this, in the study area the evidence of different colluvial deposits in these pedosequences shares similarities with cover-beds successions (Kleber and Terhorst, 2013), thought at a much smaller scale and magnitude.

4.4. Reconstruction of the environmental changes during the Holocene along the Mt. Cusna NW slope

From the pure pedogenetic point of view, three separate phases have been recorded inside the soil units all along the slope (fig. 7). From the oldest to the most recent, they are identified as:

- *α pedogenesis*: it is observed exclusively in unit II of 02 (and partially in unit III of 06), and displays the characteristics of a well-developed brunification with clay illuviation (Duchaufour, 1983). This strongly expressed pedogenetic phase led to the formation of a Luvisol (IUSS Working Group WRB, 2015), developed under a forest vegetation cover, as evidenced by the yellowish brown matrix with speckled striated b-fabric (Douglas and Thompson, 1985) and by the pedofeatures (i.e., frequent typic clay coatings; rare crescent typic clay coatings; very few typic clay infillings) observed in thin sections. This phase was interrupted by a sudden deposition of colluvial material, mobilized upslope by water runoff. During this phase, the soil surface of the evolving soil was buried, interrupting its pedogenesis. During this runoff period, the slope was not likely covered by forests, as they would have effectively prevented such mass movements. Consequently, this colluvial event provided a new parent material for further soil development during the following phase;

- *β pedogenesis*: it is characterized by a moderately developed brunification with some clay illuviation (i.e., unit I of 02, unit II of 01, 05, and probably 03 and unit II of 06) in different parent materials. The presence of different parent materials is probably the results not only of various colluvial events, but also of a differentiated material deposition, both in quantity and composition, due to variable distance from the source and slope characteristic (e.g., steepness). The pedological characteristics of this second phase, comparatively to the first phase but in a lesser extent, point to the formation of Luvisols (IUSS Working Group WRB, 2015) under a stable forest cover. Similarly, a second colluvial event interrupted this pedogenetic phase. However, in this case, the deposited material is more homogeneous, as it is mainly composed of claystone fragments (including lithorelicts *sensu* Brewer, 1976) and pedorelicts (*sensu* Brewer, 1976), coming from the B horizons of Luvisols developed during the former pedogenetic phase, then eroded and reworked by geomorphological processes.

- *γ pedogenesis*: the characteristics of the present-day pedogenetic phase suggest a slight change in conditions compared to the previous two phases. The values of the $Al_o + ½ Fe_o$ index calculated for ABt2 and BC horizons of 02 profile seem to evidence a weak podzolization (Do Nascimento et al., 2008; Waroszewski et al., 2013; IUSS Working Group WRB, 2015). However, this process is not recognizable in the field, and is therefore qualified as cryptopodzolization, forming a "ranker cryptopodzolique" soil (*sensu* Duchaufour, 1983) or a Leptosol (protospodic) (IUSS Working Group WRB, 2015), as already observed in other soils of the Mt Cusna (Mariani, 2016). This process could be favored by the development of low shrub vegetation dominated by *Vaccinium myrtillus* (Duchaufour, 1983; Chersich et al., 2007; Compostella et al., 2013; Mariani, 2016). As far as the other profiles are concerned, under the same vegetation cover, an even less conspicuous process than cryptopodzolization can act, inducing the formation of a "ranker subalpin" soil (Duchaufour, 1983) or an Umbric Leptosol (IUSS Working Group WRB, 2015), except for the 04 profile, located downslope in a forest context, which can be regarded as a "ranker brunifié" soil (Duchaufour, 1983) or a Brunic Leptosol (IUSS Working Group WRB, 2015).

Finally, in some cases, the present-day pedogenesis is superimposed to the previous one (see section 4.2 of the Discussion), the latter being identifiable by relict and textural pedofeatures (see section 4.2 of the Discussion), emphasizing a greater inertia (Duchaufour, 1983) than the ongoing pedofeatures development.

4.5. Interactions between the geomorphological context, the Holocene climate variations, and the vegetation changes as influencing factors on paleosols

The study area is characterized during the Holocene by alternating phases of rhexistasy and biostasy (Erhart, 1967). The pedogenesis has been mainly affected by three factors throughout time (i.e., climate, vegetation, slope features), which strongly influenced the environmental evolution of the area. In Fig. 9, a sketch on the role of the main factors influencing the soil development through time in the study area is proposed and herein discussed. The most ancient phase, recorded by the paleosols, was a biostasy phase (α pedogenesis) during which the climate was probably warm with a stable forest vegetation cover at the Mt. Cusna NW slope. Soil processes were mainly governed by a well-developed brunification, together with clay illuviation. Even if the time control of the pedogenetic phases at Mt. Cusna area remains speculative, it is likely that this pedogenetic phase took place before the Early Holocene (see below). Subsequent climate changes and their associated vegetation shift downward the slope caused a phase of strong instability, marked by the action of colluvial processes and the interruption of pedogenetic processes. In the Apennines, a relationship can be drawn between cold periods and an increase in landslides and slope movements (Bertolini, 2007). During such a phase, slope processes eroded soils and deposited un-weathered mineral material at the topographic surface. The change to warmer temperatures promoted a new stable phase (β), characterized by similar environmental conditions observed during the previous warm period. According to Compostella et al. (2013) and Cremaschi et al., (1984), this phase could correspond to the Early/Middle Holocene, since in the neighboring area, the charcoals coming from the upper part of soils developed during the β pedogenesis were radiocarbon dated (3920-3700 cal yr BP: Compostella et al., 2013) after the Middle/Late Holocene boundary, near the transition between Subboreal and Subatlantic periods (Mariani et al., 2019). The difference in soil development grade, in respect to the previous stable phase, can be attributed to the different duration of pedogenesis or to a different vegetation cover, as testified by the variation in organic material characteristics highlighted by Rock-Eval analysis. This stability phase was interrupted by slope instability, due to a likely climate deterioration (probably during the LIA, Mariani et al., 2019) associated to a loss of the vegetation cover. However, colluvial processes during this latter phase of rhexistasy seem to have been less intense than the previous one, with soils partially eroded, and in some case, with previously buried paleosols exhumed. Moreover, transported and deposited material was often pre-altered, as it was originating from paleosols developed in higher topographic positions. Finally, the present-day pedogenesis starts from these colluvial deposits and/or from the exhumed paleosols. The present-day phase of biostasy (γ) is characterized by distinctive environmental conditions with a different vegetation cover (i.e., shrubs): present-day soils are apparently less developed, possibly because of the vegetation type (i.e., cryptopodzolization induced by *Vaccinium myrtillus*), colder conditions, or a short duration of pedogenesis (Duchaufour, 1983; Compostella et al., 2014). The sparse vegetation cover, mainly composed of shrubs, does not protect the soil enough from water driven erosion acting today, triggering a soil cover erosion along the edge of rills.

5. Conclusions

This paper presented the assessment of the different environmental conditions that affected the NW slope of Mt. Cusna, based on the analysis of soils and paleosols. In the Mt. Cusna toposequence, three different soil units have been identified: (i) a first (and the most ancient) soil unit, characterized by a well-developed brunification with clay illuviation, (ii) a second unit, characterized by the same processes of the first unit, but less intense, and (iii) a third recent unit, presenting a weak pedogenesis. This latter, in some case, superimposed on an older truncated soil (paleosol), affecting these exhumed paleosols. Based on the study of these soil units, it has been possible to reconstruct environmental changes that affected the Mt. Cusna slope during the Holocene, to identify the succession of phases of slope stability, during which soils developed, and phases characterized by erosion and deposition processes.

In this light, soils proved to be a useful archive, not only to reconstruct the past environmental conditions, but also to trace the geomorphological processes that affected the area. In addition, it has been possible to identify the role of the geomorphological processes that have affected the evolution of complex paleosol sequences. This work, based on different lab techniques, demonstrated that a multi-analytical approach is necessary to properly characterize soils and their genetic pedological processes; for example, the use of Rock-Eval analysis improved substantially our knowledge about the relationship between paleosols and organic matter and, as such, opens new research avenues in paleopedogenesis.

Acknowledgments

The authors are grateful to Dr. Compostella and Dr. Ferrari for their assistance in laboratory analyses.

References

Albrecht, R., Sebag, D., Verrecchia, E.P., 2015. Organic matter decomposition: bridging the gap between Rock–Eval pyrolysis and chemical characterization (CPMAS 13C NMR). Biogeochemistry 122, 101–111.

Arduino, E., Barberis, E., Ajmone Marsan, F., Zanini, E., Franchini, M., 1986. Iron oxides and clay minerals within profiles as indicators of soil age in northern Italy. Geoderma, 37, 45—55.

Avery, B. W., Bascomb, C. L., (Eds.). 1982. Soil survey laboratory methods. Lawes agricultural trust.

Bascomb, C. L., 1968. Distribution of pyrophosphate-extractable iron and organic carbon in soils of various groups. European Journal of Soil Science, 19(2), 251-268.

Behar, F., Beaumont, V., De B. Penteado, H.L., 2001. Rock-Eval 6 technology: performances and developments. Oil & Gas Science and Technology 56 (2), 111–134.

Biagi, P., Castelletti, L., Cremaschi, M., Sala, B., Tozzi, C., 1980. Popolazione e territorio nell'Appennino ToscoEmiliano e nel tratto centrale del bacino del Po e nelle Prealpi bresciane tra il IX ed il V millennio. Emilia Preromana, 8, 13–36.

Bertolini, G., 2007. Radiocarbon dating on landslides in the Northern Apennines (Italy). In: McInnes R., Jakeways J., Fairbank H., Mathie E., (eds), Landslides and Climate Change. Taylor & Francis Group, London.

Bertolini, G., Pellegrini, M., 2001. The landslides of Emilia Apennines (Northern Italy) with reference to those which resumed activity in the 1994–1999 period and required civil protection interventions. Quaderni di Geologia, 8(1), 27–74.

Bollati, I. M., Masseroli, A., Mortara, G., Pelfini, M., Trombino, L., 2019. Alpine gullies system evolution: erosion drivers and control factors. Two examples from the western Italian Alps. Geomorphology, 327, 248-263.

Bortolotti, V., 1992. Guide Geologiche Regionali: Appennino Tosco-Emiliano. Milano: BE-MA Editrice.

Brewer, R., 1976. Fabric and Mineral Analysis of Soils. Huntington, NY: Krieger.

Casagrande, A., 1934. Die Aräometer-Methode zur Bestimmung der Kornverteilung von Böden und anderer Materialien. – Springer, Berlin, 56 p.

Chersich, S., Galvan, P., Frizzera, L., Scattolin, L., 2007. Variabilità delle forme di humus in due siti campione di pecceta altimontana trentina. Forest@-Journal of Silviculture and Forest Ecology, 4 (2), 220-226.

Coltorti, M., Pieruccini, P., 2006. The last interglacial pedocomplexes in the litho-and morpho-stratigraphical framework of the central-northern Apennines (Central Italy). Quaternary International, 156, 118-132.

Coltorti, M., Pieruccini, P., Arthur, K. J., Arthur, J., Curtis, M., 2019. Geomorphology, soils and palaeosols of the Chencha area (Gamo Gofa, south western Ethiopian Highlands). Journal of African Earth Sciences, 151, 225-240.

Compostella, C., Mariani, G.S., Trombino, L., 2014. Holocene environmental history at the treeline in the Northern Apennines, Italy: A micromorphological approach. The Holocene, 24(4), 393–404.

Compostella, C., Trombino, L., Caccianiga, M., 2013. Late Holocene soil evolution and treeline fluctuations in the Northern Apennines. Quaternary International, 289, 46–59.

Cremaschi M., Rodolfi, G., 1991. Il suolo - Pedologia nelle scienze della Terra e nella valutazione del territorio. La Nuova Italia Scientifica, Roma.

Cremaschi, M., Trombino, L., Zerboni, A., 2018. Palaeosoils and relict soils: a systematic review. In Interpretation of Micromorphological Features of Soils and Regoliths (pp. 863-894). Elsevier.

Cremaschi, M., Biagi, P., Accorsi, C.A., Bandini Mazzanti, M., Rodolfi, G., Castelletti, L., Leoni, L., 1984. Il sito mesolitico di Monte Bagioletto (Appennino Reggiano) nel quadro delle variazioni ambientali oloceniche dell'Appennino Tosco-Emiliano. Emilia Preromana, 9/10, 11-46.

D'Amico, M. E., Catoni, M., Terribile, F., Zanini, E., Bonifacio, E., 2016. Contrasting environmental memories in relict soils on different parent rocks in the south-western Italian Alps. Quaternary International, 418, 61-74.

Dewolf, Y., Bourrié, G., 2008. Les formations superficielles: genèse, typologie, classification, paysages et environnements, ressources et risques. Ellipses.

Do Nascimento, N. R., Fritsch, E., Bueno, G. T., Bardy, M., Grimaldi, C., Melfi, A. J., 2008. Podzolization as a deferralitization process: dynamics and chemistry of ground and surface waters in an Acrisol–Podzol sequence of the upper Amazon Basin. European Journal of Soil Science, 59(5), 911-924.

Douglas, L. A., Thompson, M. L., 1985. Soil micromorphology and soil classification. Madison, WI: Soil Science Society of America.

Duchaufour, P., 1983. Pédologie. 1. Pédogenèse et classification. Masson, Paris.

Erhart, H., 1967. La Genèse des sols en tant que phénomène géologique: esquisse d'une théorie géologique et géochimique, biostasie et rhexistasie: exmaples d'application. Masson.

Fedoroff, N., Courty, M., 2012. Textural features and microfacies expressing temporary and permanent soil water saturation. In Poch-Claret, R., Casamitjana, M., and Francis, M., editors, Proceedings of the 14th Intern. Working Meet. On Soil Micromporphology, page 1.1.K. Session I. Editions i Publications de la Universitat de Lleida, Spain.

Fedoroff, N., Goldberg, P., 1982. Comparative micromorphology of two late Pleistocene paleosols (in the Paris Basin). Catena, 9, 227-251.

Gales, S.J., Hoare, P.G., 1991. Quaternary Sediments: Petrographic Methods for the Study of Unlithified Rocks Belhaven, London, p. 323

Giraudi, C., 2005. Middle to Late Holocene glacial variations, periglacial processes and alluvial sedimentation on the higher Apennine massifs (Italy). Quaternary Research, 64(2), 176-184.

IUSS Working Group WRB, 2015. World Reference Base for Soil Resources 2014, update 2015 International soil classification system for naming soils and creating legends for soil maps. World Soil Resources Reports No. 106. FAO, Rome.

Jenny, H., 1941. Factors of soil formation: a system of quantitative pedology. McGraw-Hill book company inc., New York.

Jahn, R., Blume, H. P., Asio, V. B., Spaargaren, O., Schad, P., 2006. Guidelines for soil description. FAO.

Kaiser, K., Schoch, W. H., Miehe, G., 2007. Holocene paleosols and colluvial sediments in Northeast Tibet (Qinghai Province, China): properties, dating and paleoenvironmental implications. Catena, 69(2), 91-102.

Kemp, R.A., 1998. Role of Micromorphology in paleopedological research. Quaternary International 51-52, 133-141.

Kjeldahl, J., 1883. Neue Methode zur Bestimmung des Stickstoffs in organischen Körpern. J. Anal. Chem. 22, 366–382.

Kleber, A., Terhorst, B., 2013. Mid-latitude slope deposits (cover beds) (Vol. 66). Newnes.

Krasilnikov, P., Calderón, N.E.G., 2006. A WRB-based buried paleosol classification. Quaternary International, 156, 176-188.

Kubiëna, W.L., 1953. Bestimmungsbuch und Systematik der Böden Europas. F. Enke Verlag, Stuttgart.

Lafargue, E., Marquis, F., Pillot, D., 1998. Rock-Eval 6 applications in hydrocarbon exploration, production, and soil contamination studies. Oil & Gas Science and Technology 53 (4), 421–437.

Losacco, U., 1949. La glaciazione quaternaria dell'Appennino Settentrionale. Rivista Geografica Italiana, 56(2), 90-152.

Losacco, U., 1982. Gli antichi ghiacciai dell'Appennino settentrionale. Studio morfologico e paleogeografico. Atti della Societa dei Naturalisti e Matematici di Modena, 113, 1–24.

Magliulo, P., Terribile, F., Colombo, C., Russo, F., 2006. A pedostratigraphic marker in the geomorphological evolution of the Campanian Apennines (Southern Italy): The Paleosol of Eboli. Quaternary international, 156, 97-117.

Mariani, G. S., Compostella, C., Trombino, L., 2019. Complex climate-induced changes in soil development as markers for the Little Ice Age in the Northern Apennines (Italy). Catena, 181, 104074.

Mariani, G. S., Cremaschi, M., Zerboni, A., Zuccoli, L., Trombino, L., 2018. Geomorphology of the Mt. Cusna Ridge (Northern Apennines, Italy): evolution of a Holocene landscape. Journal of Maps, 14(2), 392-401.

Mariani, G.S., 2016. The role of paleosols in paleoenvironmental studies: genesis and development of Apennine mountain soils during the Holocene. Phd Thesis, University of Milan.

Matteodo, M., Grand, S., Sebag, D., Rowley, M. C., Vittoz, P., Verrecchia, E. P., 2018. Decoupling of topsoil and subsoil controls on organic matter dynamics in the Swiss Alps. Geoderma, 330, 41-51.

McCarthy P.J., Martini, I.P., Leckie, D.A., 1998. Use of micromorphology for palaeoenvironmental interpretation of complex alluvial palaeosols: an example from the Mill Creek Formation (Albian), southwestern Alberta, Canada. Palaeogeography, Palaeoclimatology, Palaeoecology 143, 87-110.

Milne, G., 1936. Normal erosion as a factor in soil profile development. Nature, 138(3491), 548.

Ministero delle Risorse Agricole Alimentari e Forestali, 1994. Metodi ufficiali di 1036 analisi chimica del suolo, con commenti ed interpretazioni. ISMEA, Roma, 207 pp.
Nicosia, C., 2006. Indicatori micromorfologici di erosione dei suoli nel settore settentrionale delle Valli Grandi Veronesi durante l'età del Ferro. Padusa, 62, 108-112.
Panizza, M., Bettelli, G., Bollettinari, G., Carton, A., Castaldini, D., Piacente, S., Bernini, M., Clerici, A., Tellini, C., Vittorini, S., Canuti, P., Moisello, U., Tenti, G., Dramis, F., Gentili, B., Pambianchi, G., Bidini, D., Lulli, L., Rodolfi, G., Busoni, E., Ferrari, G., Cremaschi, M., Marchesini, A., Accorsi, C.A., Mazzanti, M., Francavilla, F., Marchetti, G., Vercesi, P.L., Di Gregorio, F., Marini, A., (Gruppo Ricerca Geomorfologia CNR) 1982. Geomorfologia del territorio di Febbio tra il M.Cusna e il F.Secchia (Appennino Emiliano). Geografia Fisica Dinamica Quaternaria, 5, 285-360.
Pawluk, S., 1972. Measurement of crystalline and amorphous iron removal in soils. Can.. J. Soil Sci. 52: l19-123.
Rellini, I., Trombino, L., Firpo, M., Piccazzo, M., 2007. Geomorphological context of "plinthitic paleosols" in the Mediterranean region: examples from the coast of western Liguria (northern Italy).Rev. C. & G., 21 (1-2), 27-40.
Rhodes, E. R., Sutton, P. M., 1978. Active iron ratio of some soils from three physiographic units in Sierra Leone. Soil Science, 125(5), 326-328.
Ruellan, A., 1971. The history of soils. Some problems of definition and interpretation. In: Yaalon, D.H. (Ed.), Paleopedology. Origin, Nature and Dating of Paleosols. Israel University Press, Jerusalem, 350 pp.
Sauro, U., Ferrarese, F., Francese, R., Miola, A., Mozzi, P., Rondo, G.Q., Trombino, L., Valentini, G., 2009. Doline fills- case study of the Faverghera Plateau (Venetian Pre-Alps, Italy). Acta Carsologica, 38 (1), 51-63.
Schomburg, A., Verrecchia, E. P., Guenat, C., Brunner, P., Sebag, D., Le Bayon, R. C., 2018. Rock-Eval pyrolysis discriminates soil macro-aggregates formed by plants and earthworms. Soil Biology and Biochemistry, 117, 117-124.
Schomburg, A., Sebag, D., Turberg, P., Verrecchia, E. P., Guenat, C., Brunner, P., Adatte T, Schlaepfer R., Le Bayon, R. C., 2019. Composition and superposition of alluvial deposits drive macro-biological soil engineering and organic matter dynamics in floodplains. Geoderma, 355, 113899.
Schwertmann, U., 1973. Use of oxalate for Fe extraction from soils. Canadian Journal of Soil Science, 53(2), 244-246.
Sebag, D., Verrecchia, E. P., Cécillon, L., Adatte, T., Albrecht, R., Aubert, M., Bureau, F., Cailleau, G., Copard, Y., Decaens, T., Disnar, J. R., Hetényi, M., Nyilas, T., Trombino, L., 2016. Dynamics of soil organic matter based on new Rock-Eval indices. Geoderma, 284, 185-203.
Sheldon, N.D., Tabor, N.J., 2009. Quantitative paleoenvironmental and paleoclimatic reconstruction using paleosols. Earth-Science Reviews, 95(1-2), 1-52.
Stoops, G., 2003. Guidelines for analysis and description of soil and regolith thin sections. Soil Science Society of America, Inc., Madison, Wisconsin, USA.
Stoops, G., Marcelino, V., Mees, F., 2018. Interpretation of micromorphological features of soils and regoliths. Elsevier.
Stoops, G., Marcelino, V., Mees, F., 2010. Interpretation of micromorphological features of soils and regoliths. Elsevier.
Vittori Antisari, L., Bianchini, G., Cremonini, S., Di Giuseppe, D., Falsone, G., Marchesini, M., Marvelli, S., Vianello, G., 2016. Multidisciplinary study of a late glacial-Holocene sedimentary sequence near Bologna (Italy): insights on natural and anthropogenic impacts on the landscape dynamics. J. Soils Sediments 16, 645-662.
Walkley, A., Black, I.A., 1934. An examination of the Degtjareff method for determining soil organic matter, and proposed modification of the chromic acid titration method. Soil Sci, 37(1), 29-38.
Waroszewski, J., Kalinski, K., Malkiewicz, M., Mazurek, R., Kozlowski, G., Kabala, C., 2013. Pleistocene–Holocene cover-beds on granite regolith as parent material for Podzols—an example from the Sudeten Mountains. Catena, 104, 161-173.
Zanelli, R., Egli, M., Mirabella, A., Giaccai, D., Abdelmoula, M., 2007. Vegetation effects on pedogenetic forms of Fe, Al and Si and on clay minerals in soils in southern Switzerland and northern Italy. Geoderma, 141(1-2), 119-129.

Zanini, E., Freppaz, M, Stanchi, S, Bonifacio, E, Egli, M., 2015. Soil variability in mountain areas. In: Romeo, R; Vita, A; Manuelli, S; Zanini, E; Freppaz, Michele; Stanchi, Silvia. Understanding Mountain Soils: A Contribution from mountain areas to the International Year of Soils 2015. Rome: FAO, 60-62.

Tables

Table 1.

Profile	Elevation (m a.s.l.)	Slope gradient (°)	Slope exposure	Profile exposure	Parent Material	Geomorphological context	Vegetation
01	1680	10	NE	SW	Colluvium deposits composed of claystones	Middle slope affected by running water erosion	Semi-deciduous shrub
02	1669	2	N-NW	SW	Colluvium deposits composed of claystones	Middle slope affected by running water erosion	Semi-deciduous shrub
03	1665	4	NW	N	Colluvium deposits composed of claystones	Middle slope affected by running water erosion	Semi-deciduous shrub
04	1659	11	NW	N-NE	Colluvium deposits composed of claystones	Middle slope affected by running water erosion	Deciduous woodland
05	1663	10	NW	N-NE	Colluvium deposits composed of claystones	Middle slope affected by running water erosion	Semi-deciduous shrub
06	1661	22	S-SE	SW	Colluvium deposits composed of claystones	Middle slope	Semi-deciduous shrub

Table 1. Site description of investigated soil profiles.

Table 2.

Profile	Horizon	Depth (cm)	Fe_o (g/g)	Al_o (g/kg)	Fe_d (g/kg)	Al_d (g/kg)	Fe_p (g/kg)	Al_p (g/kg)	Fe_{cry} (Fe_d-Fe_o) g/kg	Feo/Fed	Al_o+1/2Fe_o %
01	O	0-4	6.24	2.87	15.16	3.65	4.70	11.41	8.91	0.41	0.60
	A1	4-10	6.33	3.46	16.39	4.09	5.81	8.67	10.06	0.39	0.66
	A2	10-31	6.84	3.29	21.99	4.88	6.24	10.90	15.15	0.31	0.67
	BC	31-35	9.08	4.40	17.78	4.13	5.54	6.62	8.70	0.51	0.89
	2AB1	35-44	9.52	2.74	25.98	4.37	9.70	8.50	16.46	0.37	0.75
	2AB2	44-65	15.73	4.44	31.47	5.71	15.98	10.37	15.74	0.50	1.23
	2Bw	65-80	9.84	5.06	17.39	5.05	7.44	7.46	7.55	0.57	1.00
	2Bt	80-100	3.85	2.88	16.20	4.97	4.10	6.09	12.35	0.24	0.48
	2BC1	100-120	5.80	4.30	12.17	4.17	<3.00	4.86	6.37	0.48	0.72
	2BC2	120-140+	4.19	3.45	11.82	4.00	n.d.	3.99	7.63	0.35	0.55
02	OB	0-20	11.49	4.02	22.76	4.44	8.68	7.46	11.27	0.50	0.98
	ABt1	20-60	5.73	3.45	17.01	5.16	n.d.	6.92	11.29	0.34	0.63
	ABt2	60-75	2.48	3.16	12.12	3.17	n.d.	3.84	9.64	0.20	0.44
	BC	75-95	8.82	5.40	13.37	3.62	n.d.	4.57	4.55	0.66	0.98
	2AB	95-121	<0.90	1.69	12.70	3.07	n.d.	3.32	n.d.	n.d.	n.d.
	2Btg	121-151	n.d.	0.85	14.35	3.27	n.d.	3.64	n.d.	n.d.	n.d.
	3AB	151-176+	3.48	2.40	12.14	2.84	n.d.	2.98	8.66	0.29	0.41
03	OA	0-8	7.73	3.39	20.43	4.10	6.21	7.08	12.70	0.38	0.73
	OB	8-22	10.11	2.74	30.57	4.25	12.26	9.42	20.47	0.33	0.78
	BC	22-44+	12.92	5.59	22.82	5.53	8.53	6.30	9.89	0.57	1.21
04	O	0-6	8.61	3.13	17.21	3.38	4.58	4.34	8.60	0.50	0.74
	OA	6-12	6.48	3.17	22.61	4.85	8.23	8.52	16.14	0.29	0.64
	AB	12-27	8.19	4.93	15.70	4.62	5.17	7.58	7.51	0.52	0.90
	Btg	27-54	2.82	2.64	15.57	4.53	<3.00	6.13	12.75	0.18	0.40
	Bt	54-80+	n.d.	n.d.	14.37	3.68	<3.00	4.52	n.d.	n.d.	n.d.
05	O	0-3	3.52	2.14	12.02	2.64	n.d.	3.42	8.49	0.29	0.39
	A	3-12	n.d.	n.d.	17.52	4.85	<3.00	6.53	n.d.	n.d.	n.d.
	ABt1	12-28	6.24	2.71	18.21	3.45	5.63	6.38	11.97	0.34	0.58
	ABt2	28-56+	13.06	3.78	34.13	5.83	13.27	12.09	21.08	0.38	1.03
06	O	0-6	3.52	2.12	13.44	4.02	<3.00	4.58	9.92	0.26	0.39
	OA	6-12	10.21	4.53	22.84	4.53	7.15	7.69	12.64	0.45	0.96
	2AB1	12-19	12.34	3.28	31.07	5.60	12.72	9.31	18.73	0.40	0.94
	2AB2	19-36	10.66	3.73	25.79	5.49	12.63	7.95	15.13	0.41	0.91
	2Bw1	36-54	7.28	4.39	19.03	5.72	7.54	9.21	11.76	0.38	0.80
	2Bw2	54-63	2.82	2.29	14.45	4.43	<3.00	7.30	11.63	0.20	0.37
	2Bw3	63-71	2.55	2.75	14.35	4.25	n.d.	3.92	11.80	0.18	0.40
	3AB	71-89+	5.60	3.77	13.94	3.66	n.d.	4.52	8.33	0.40	0.66

Table 2. Ammonium oxalate (Fe_o, Al_o), dithionite-citrate-bicarbonate (Fe_d, Al_d) and sodium pyrophosphate (Fe_p, Al_p) extractable Fe and Al in the studied profiles and derivate indices of crystalline iron oxides (Fe_{cry}), activity iron index (Fe_o/Fe_d) and podzolization index (Al_o+1/2Fe_o).
<: low values approximate to the minor concentration detectable; n.d.: no data.

Figure 1

Click here to download high resolution image

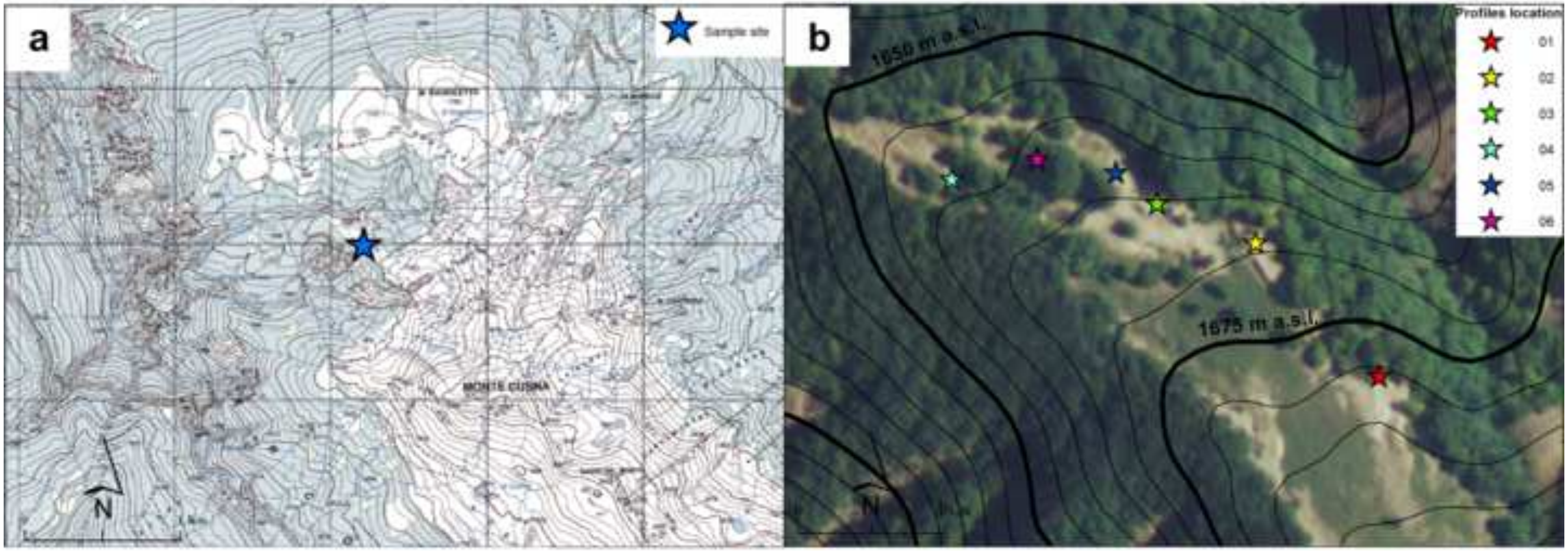

Figure 2
Click here to download high resolution image

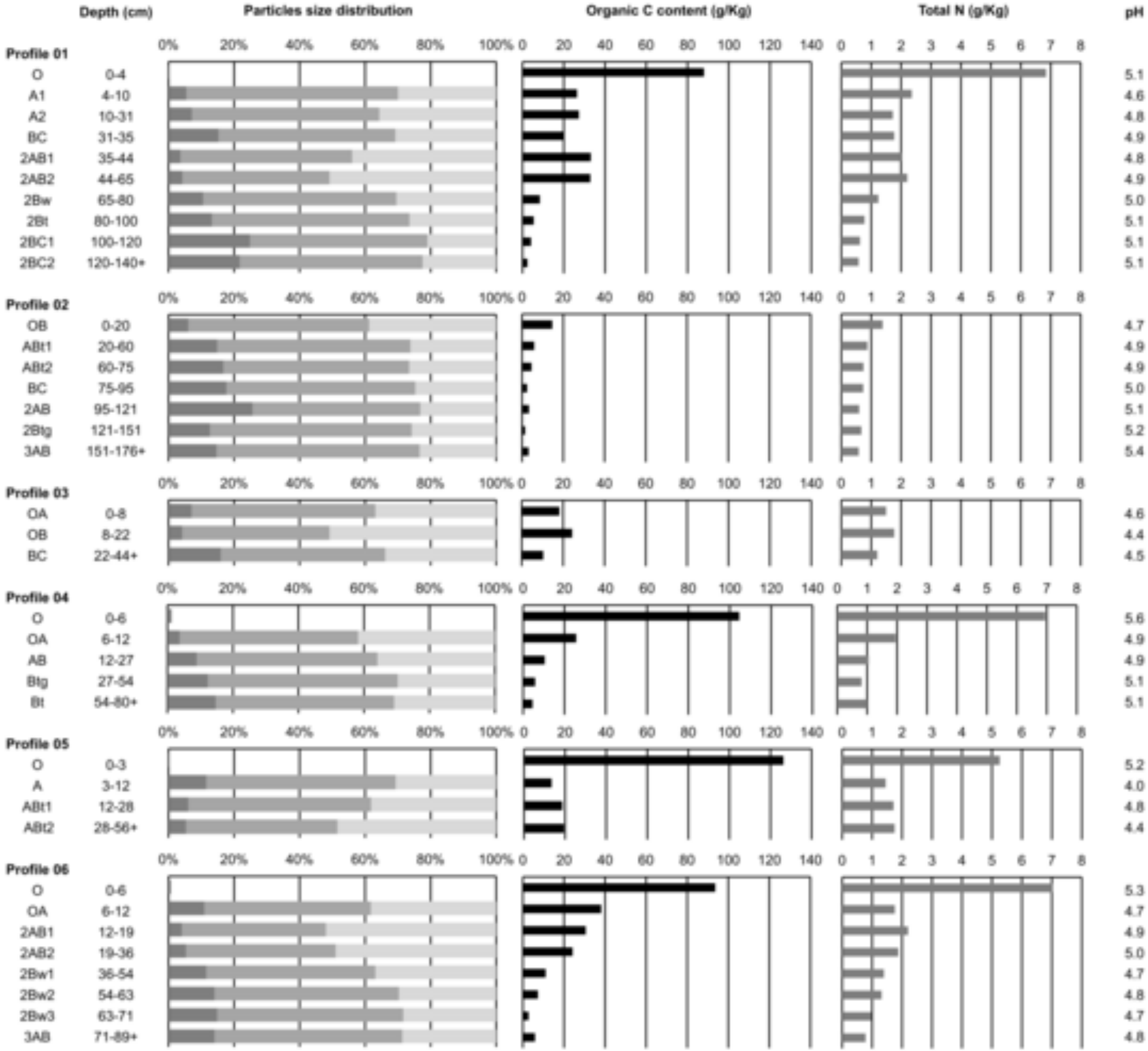

Figure 3
Click here to download high resolution image

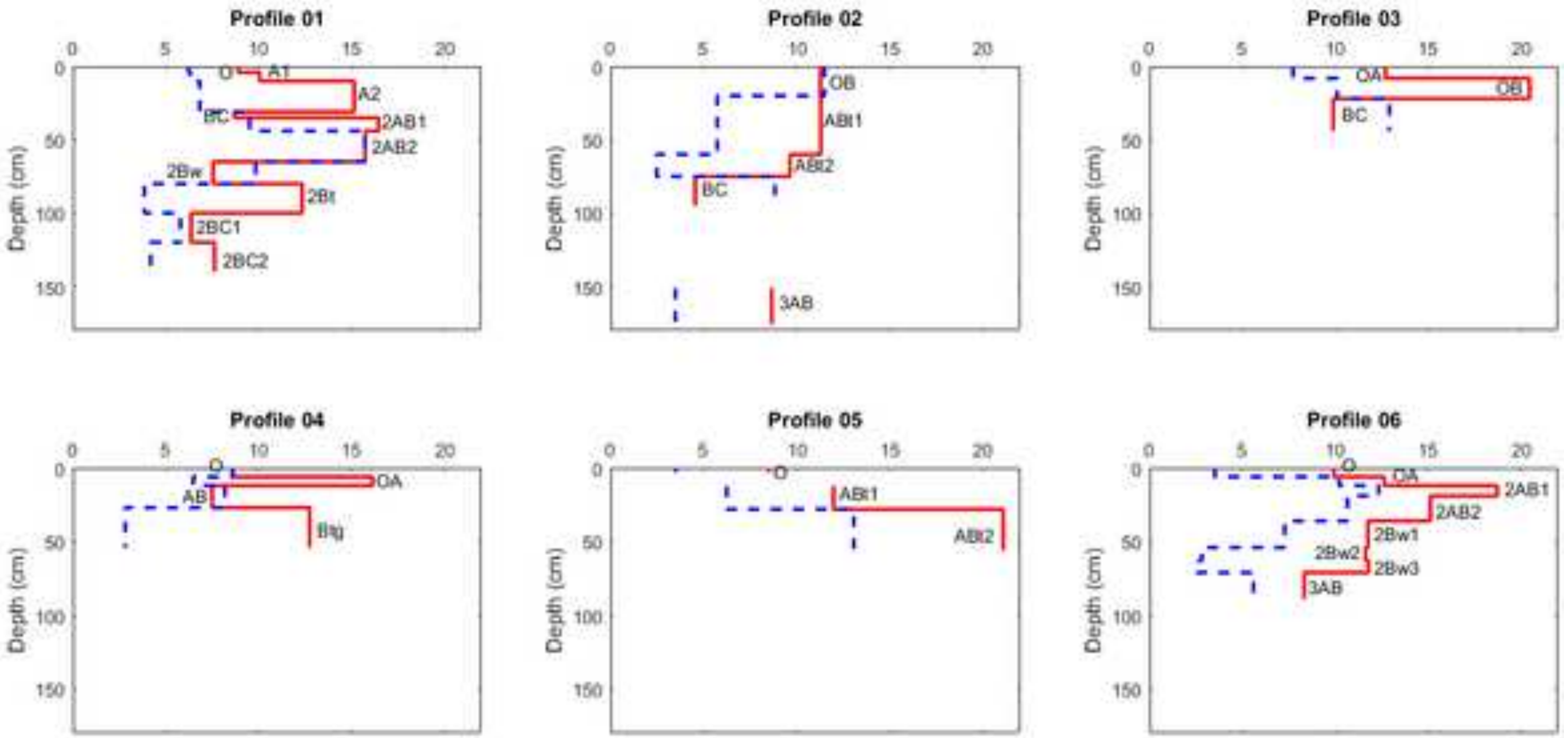

Figure 4

Click here to download high resolution image

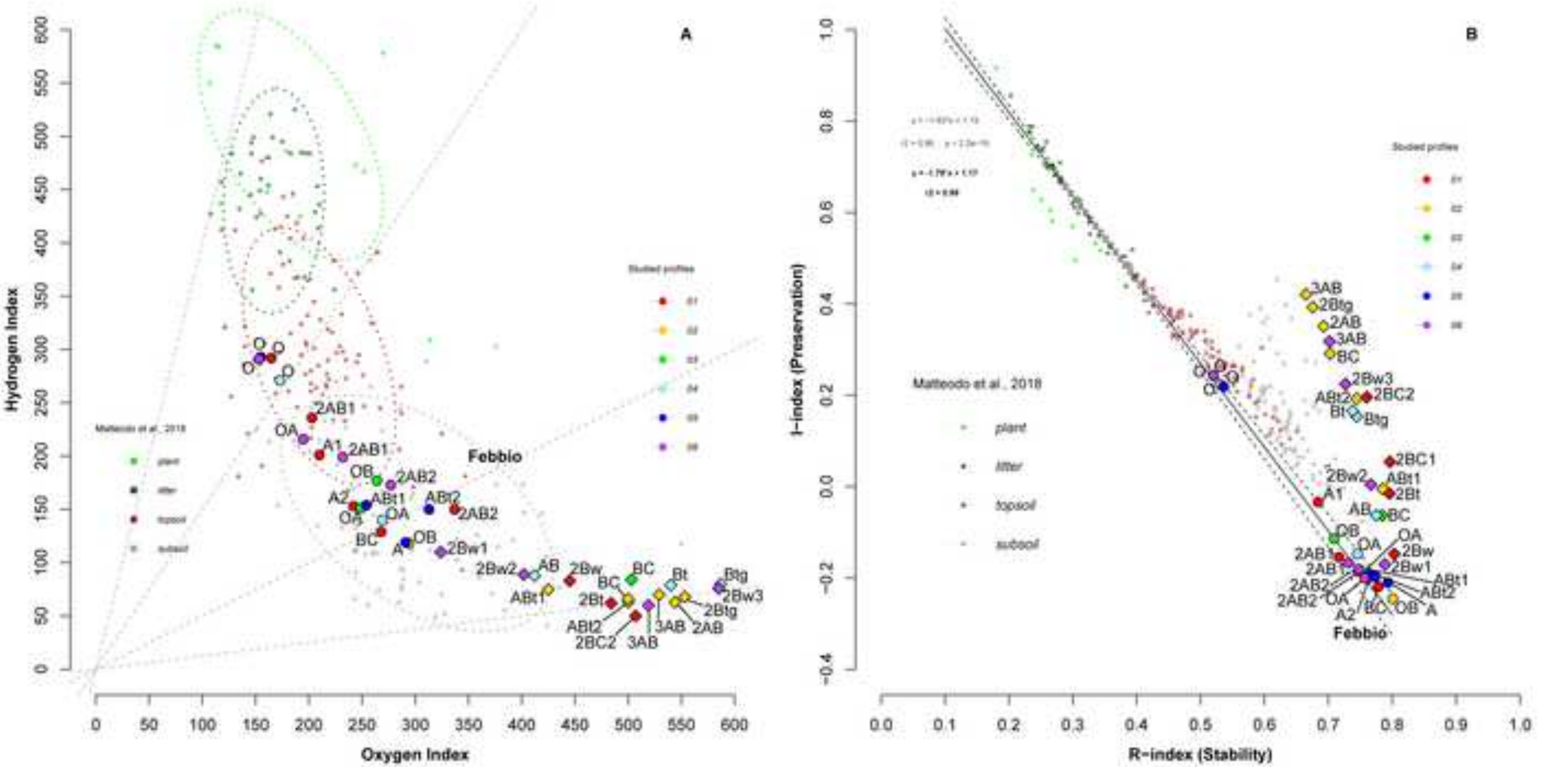

Figure 5

Click here to download high resolution image

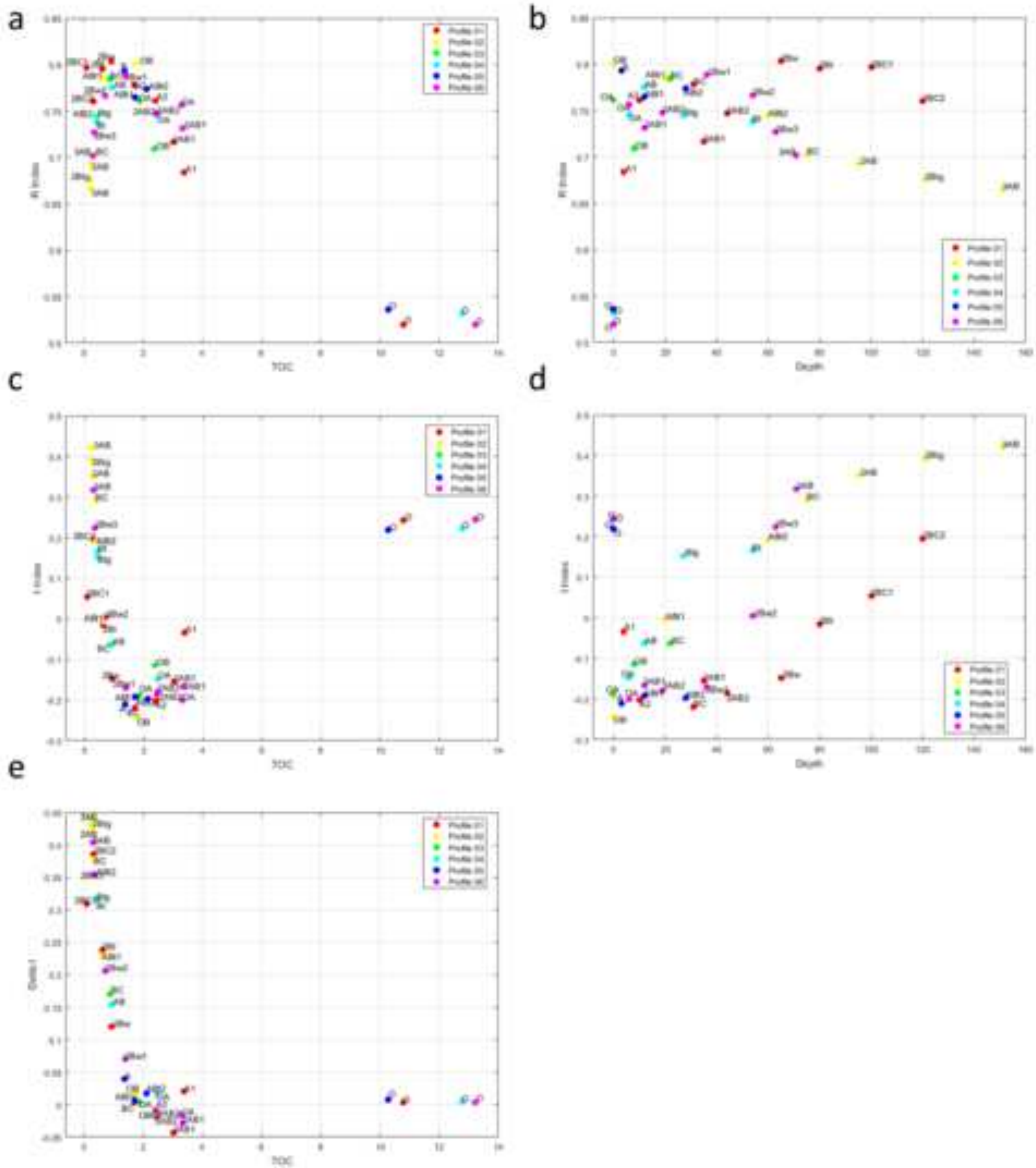

Figure 6
Click here to download high resolution image

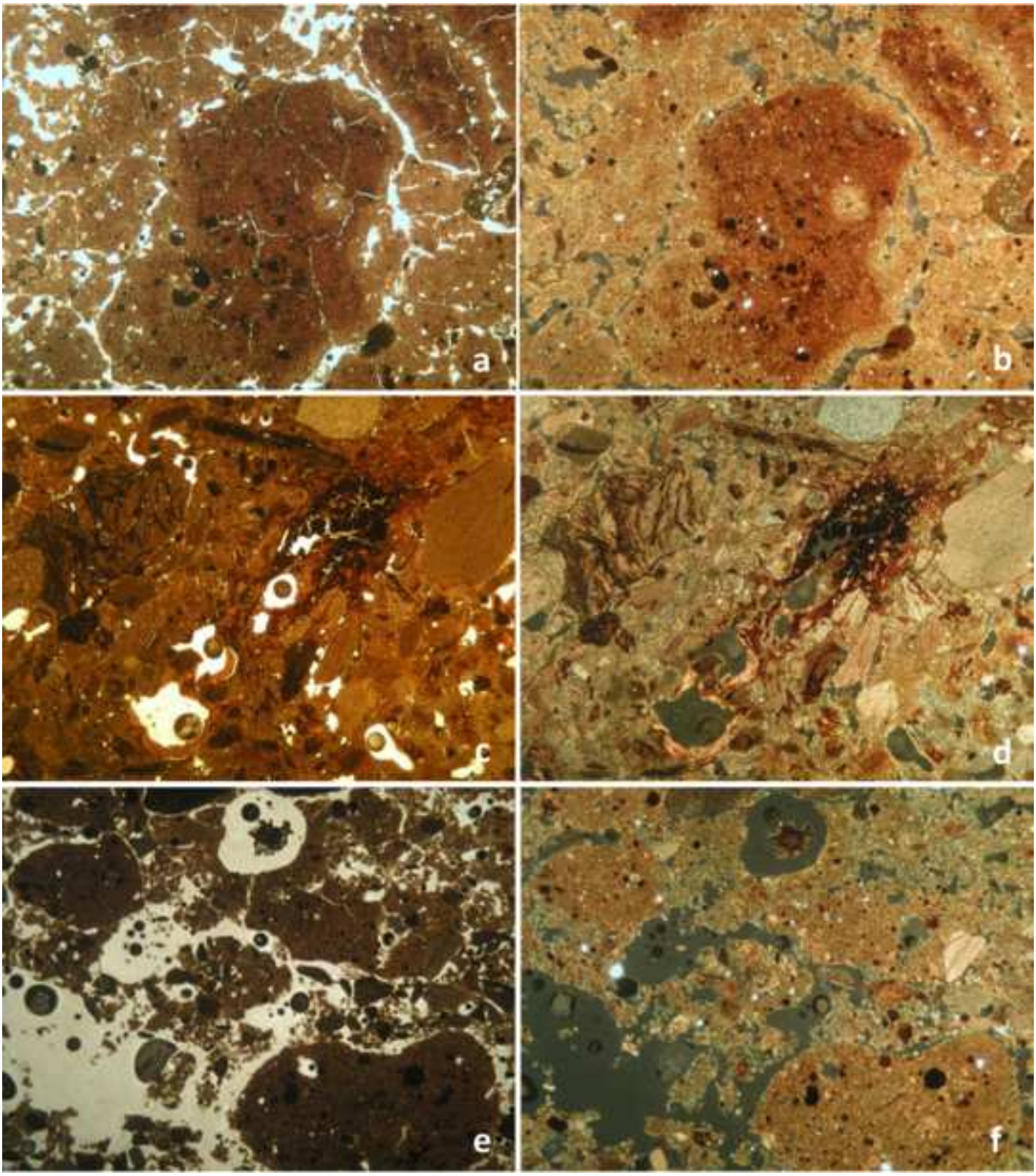

Figure 7

Click here to download high resolution image

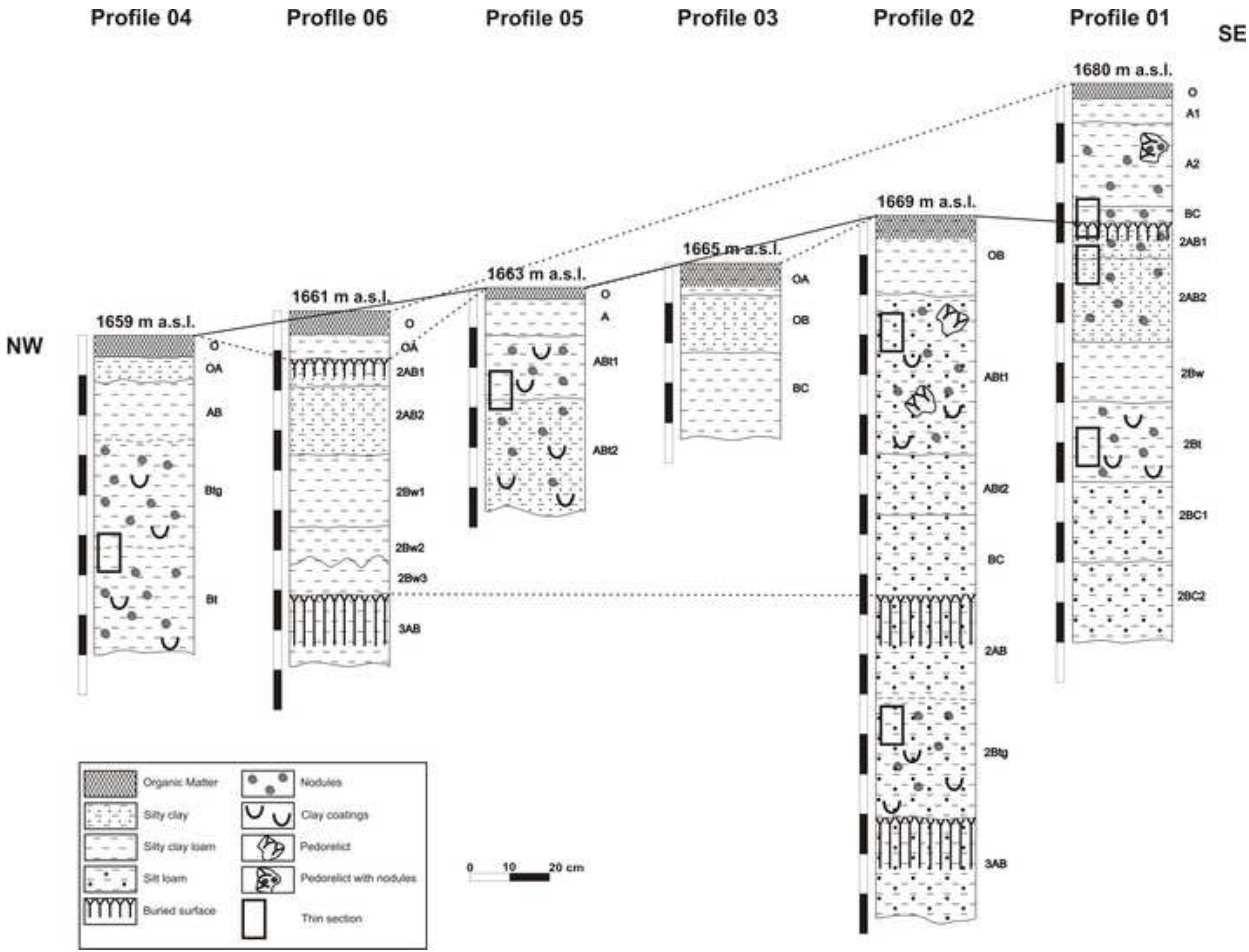

Figure 8

Click here to download high resolution image

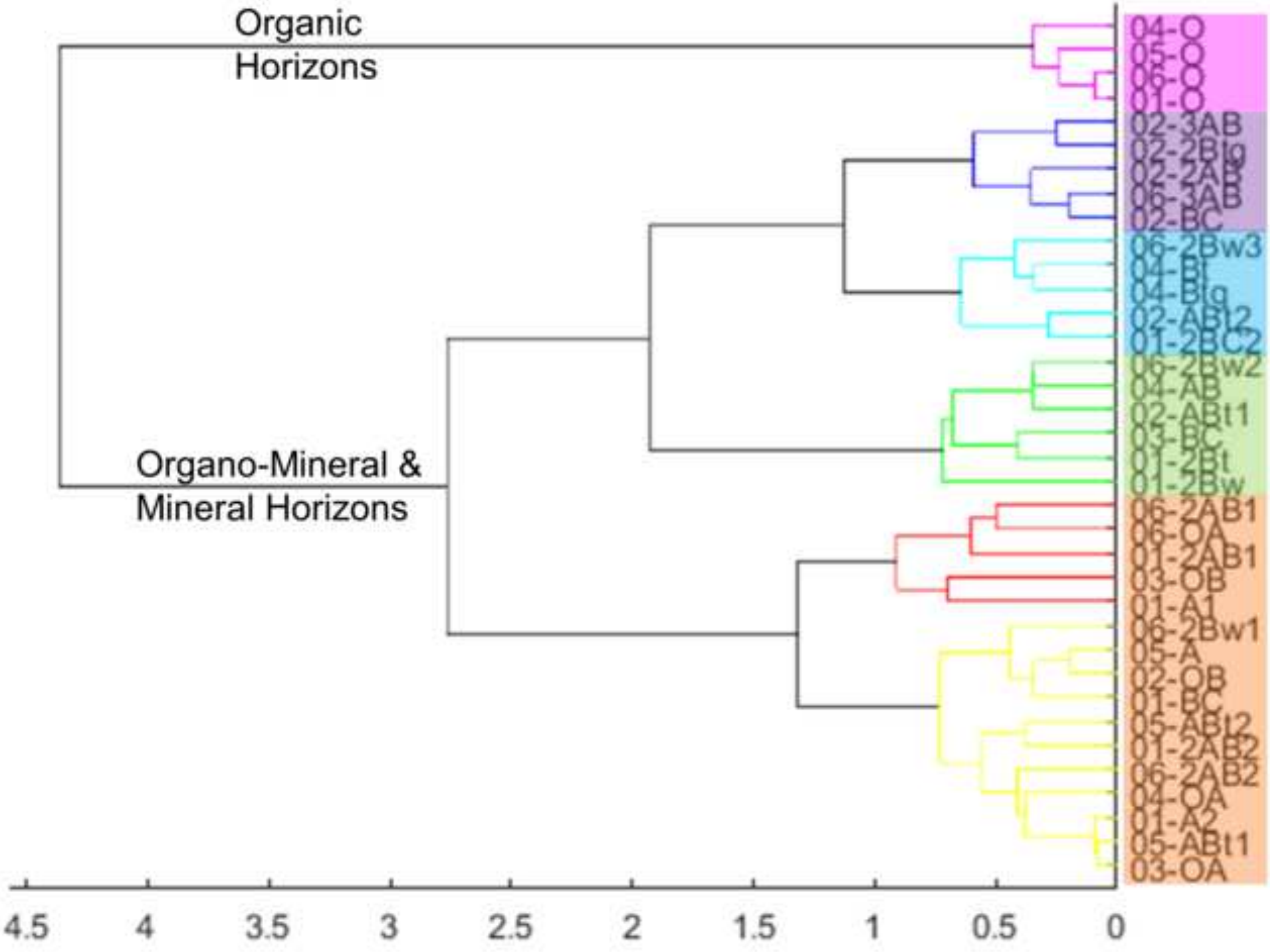

Figure 9

Click here to download high resolution image

Biorhexistasy phases	Imprints of factors		
	Climate	Vegetation	Relief
γ Biostasy phase	↑ ⊖	↕ ⊖	↕ ⊖
Rhexistasy phase	↓ ⊖	↓	↓ ⊖
β Biostasy phase	↑ ⊕	↑ ⊖	↑
Rhexistasy phase	↓ ⊕	↓	↓ ⊕
α Biostasy phase	↑ ⊕	↑ ⊕	↑

Figure Captions

Figure 1. A) Study area and location of the sample site at Mt. Cusna on altitude contour map. B) Locations of profiles on the orthophotograph (2006). The digital sources are courtesy made available by the Geoportale Nazionale (http://www.pcn.minambiente.it/GN/, WMS service).

Figure 2. Particle size distribution (dark grey: sand*; grey: silt; light grey: clay), organic C content, total N content and pH values in the studied profiles.
* Since the gravel content is very low it has been added to the sand fraction.

Figure 3. Crystalline iron oxides (Fe_{cry}, red line) and ammonium oxalate extractable Fe (Fe_o, blue dotted line) content (g/kg) in the studied profiles. The Fe_o is considered as a measure of the "activity" of the iron oxides (Schwertmann, 1973). The horizons name is given with the Fe_{cry} curves.

Figure 4. a) HI (mg HC/g TOC)/OI (mg CO2/g TOC) diagram; the horizon 01 2BC1 is not plotted due to its out of range value, b) I-index/R-index diagram of the studied horizons. Colored dots are used to calculate the "humic trend" equation written in bold. In background, the Matteodo's dataset, composed of 46 soil profiles selected across various ecounits in Swiss Alps (Matteodo et al., 2018) and the relating "humic trend" equation are depicted, as comparison.

Figure 5. a) R-Index/TOC (%) diagram; b) R-index/depth (cm) diagram; c) I-Index/TOC (%) diagram; d) I-index/depth (cm) diagram; e) Delta I/TOC (%) diagram of the studied horizons.

Figure 6. Photomicrographs of some micromorphological features observed in soils and palaeosols. a,b) altered, reddish fine-material forming subangular aggregates, with Fe/Mn nodule concentrations in 05 ABt1 and ABt2 horizons (16x, PPL e XPL; field length: 8 mm); c,d) vughy structure with clay illuviation and redoximorphic features in a 02 2Btg thin section (16x, PPL and XPL; field length: 8 mm); e,f) crumb aggregates and reddish, subangular pedorelicts in the horizon BC of the 01 profile (16x, PPL e XPL; field length: 8 mm).

Figure 7. Correlation scheme between the investigated soil profiles. The lines show the correlation among the different pedological units (black lines for the correlations found observing soil thin sections; dotted lines for the correlations supposed based on soil physical and chemical properties).

Figure 8. Dendrogram output for clustering of studied horizons, using Rock-Eval indices (HI, OI, I-Index and R-Index). The horizon 01 2BC1 is not plotted due to its out of range values.

Figure 9. Role of the main factors influencing the soil development through time in the study area. The upward arrow represents favorable conditions to soil development, whereas the downward arrow represents unfavorable conditions regarding soil development. The presence of plus or minus signs underlines the active role of a factor, which can be more (plus) or less (minus) intense, in its influence on the pedogenesis.

Appendix A

Appendix B

Appendix C

Click here to download Supplementary material for on-line publication only: Appendix C.pdf

Appendix D
Click here to download Supplementary material for on-line publication only: Appendix D.pdf

*Declaration of Interest Statement

Declaration of interests

☒ The authors declare that they have no known competing financial interests or personal relationships that could have appeared to influence the work reported in this paper.

☐The authors declare the following financial interests/personal relationships which may be considered as potential competing interests: